Universidade do Minho
Escola de Ciências da Saúde

Henrique Pedro Pereira da Silva Amaral Machado

The mechanisms underlying *Mycobacterium tuberculosis* virulence granted by the nrp gene

Mecanismos subjacentes à virulência do Mycobacterium tuberculosis conferidos pelo gene nrp.

Dissertação de Mestrado

Mestrado em Ciências da Saúde

Trabalho efetuado sob a orientação de

Doutora Margarida Saraiva

Doutor Egídio Torrado

Maio de 2015

DECLARAÇÃO

Nome: Henrique Pedro Pereira da Silva Amaral Machado

Endereço electrónico: henriquemachado@ecsaude.uminho.pt

Telefone: +351 961083628

Número do Bilhete de Identidade: 14146246

Título da dissertação: The mechanisms underlying *Mycobacterium tuberculosis* virulence granted by the nrp gene.

Orientadores:

Doutora Margarida Saraiva

Doutor Egídio Torrado

Ano de conclusão: 2015

Designação Ramo de Conhecimento do Mestrado: Ciências da Saúde

DE ACORDO COM A LEGISLAÇÃO EM VIGOR, NÃO É PERMITIDIDA A REPRODUÇÃO DE QUALQUER PARTE DESTA TESE.

Universidade do Minho, 27 de Maio de 2015

Assinatura: ____

The work presented in this dissertation was done in the Microbiology and Infection Research Domain of the Life and Health Sciences Research Institute (ICVS), School of Health Sciences, University of Minho, Braga, Portugal (ICVS/3B's – PT Government Associate Laboratory, Braga/Guimarães, Portugal).

AGRADECIMENTOS

Começo por agradecer à Doutora Margarida Saraiva. As palavras aqui escritas dificilmente conseguiriam fazer justiça à importancia que teve no meu desenvolvimente ciêntifico e pessoal ao longo dos ultimos dois anos. Sem duvida a qualidade trabalho por mim, e muitos outros, desenvolvido nos ultimos anos não teria sido atingida sem o seu esforço, dedicação e profissionalismo. Por tudo isto lhe fico imensamente grato, e desejo apenas que os próximos anos tragam ainda maior sucesso.

Quero expressar a minha gratidão ao Doutor Egídio Torrado por todo o seu empenho neste projecto. Sem dúvida o seu contributo tanto a nível científico como técnico foi essencial para levar este trabalho a bom porto. Obrigado também por todas as discussões científicas que tivemos ao longo desde último ano, sem dúvida ajudaram-me a analisar a “ciência” de forma mais critica!

Agradeço ao Doutor Apoorva Bhatt por ter disponibilizado as estirpes utilizadas neste trabalho e por ter partilhado os seus resultados preliminares. Fico também grato pela hospitalidade e prontidão com que nos recebeu em Birmingham para discutir este projecto.

Ao Professor Gil Castro, uma das primeiras pessoas que me acolheu neste instituto, queria também expressar a minha gratidão por todas as vezes que partilhou o seu vasto conhecimento cientifico comigo. Sem duvida que a sua experiência é uma mais valida para todos aqueles que trabalham à sua volta.

Gostaria também de manifestar a minha gratidão ao Professor Fernando Rodrigues por me ajudar a perceber o meu próprio trabalho de outra perspectiva, a da mycobactéria.

Ao Diogo, obrigado por tudo! Foste a primeira pessoa que me acolheu no laboratório, e sinceramente acho que nesse ponto não podia ter tido maior sorte! Ajudaste-me a dar os primeiros passos no mundo da investigação, algo que aliás te vejo a fazer ano após ano com novos estudantes sempre com o mesmo empenho. Como bem sabes este percurso nem sempre é facil, mas não tenho qualquer dúvida que ultrapassarás todos os obstáculos que encontrares. Por tudo isto, e pela constante companhia neste últimos 2 anos, muito obrigado!

À Isabel quero também expressar a minha mas sincera gratidão! Ajudaste-me em muito adquirir as competências necessárias para desenvolver este tipo de trabalho. Quantas vezes as 2 horas dentro do P3

se tornaram em 4 ou em 6? Tanto melhor, em boa companhia o tempo voa! Espero que o futuro seja repleto de alegrias, tanto profissionais como. Muito obrigado!

Hélder, não podia de forma nenhuma deixar de ter agradecer! Obrigado pela oportunidade de trabalhar no teu projecto, foi e ainda é uma aventura não só pelo valor do trabalho em si como também pela tua constante boa disposição e vontade de levar tudo a bom porto. Tenho a certeza que o futuro será brilhante!

Quero também agradecer ao Jeremy, tanto pelo trabalho que desenvolvemos juntos como pela frequente companhia dentro do P3. Muito obrigado!

Aos membros do I3.02 que fazem deste ICVS mais do que um local de trabalho, muito obrigado! Quero agradecer à Joana, Bruno, Ana Cardoso, Alice, Cláudia, Alexandra, Gabriela, Ritinha, Carine, Teresa, Ana Ribeiro, Inês, Patrícia, e Ana Belinha, algumas de vós companhias mais antigas, outras mais recentes mas sem dúvidas todas sempre prestáveis e optimas companhias! Ao Nuno, frequentemente companhia de horas tardias, um obrigado. À Flávia, Vânia e Joana Gouveia queria também deixar aqui o meu apreço. Apesar de agora trilharem diferentes percursos, ficam sempre as memórias dos bons momentos e os conselhos que por aqui deixaram, muito obrigado.

Aos meus pais posso apenas expressar a minha eterna gratidão, sendo que sem os seus esforços e por vezes privações nada disto teria sido possível. Farei tudo ao meu alcance para fazer com que todos estes anos de esforços tenham valido a pena, muito obrigado. Quero deixar também um agradecimento muito especial ao meu irmão, que desde sempre me acompanhou e apoiou. Obrigado Carlos!

Finalmente, e apesar de implícito, quero expressar a minha gratidão à Filipa. Certamente serei das pessoas mais afortunadas por ter a tua companhia neste percurso nem sempre fácil. Para mim, o teu valor é inestimável. Ajudaste-me constantemente a superar os meus próprios limites, e foste presença constante quando as coisas correram menos bem, já para não falar na ajuda prática neste mesmo trabalho! Por tudo, obrigado.

ABSTRACT

Mycobacterium tuberculosis (Mtb), the etiological agent of tuberculosis (TB), is a highly complex pathogen estimated to have caused more deaths than any other infectious agent throughout human existence. Despite global efforts to eradicate TB, this is still a leading cause of death by infectious disease, second only to the human immunodeficiency virus (HIV). Although public health measures have greatly diminished TB burden, the reality is that little has changed in anti-TB therapy and vaccination over the past decades. As an obligatory intracellular pathogen Mtb has co-evolved with its human host for over 70 thousand years. This timeframe has given Mtb ample opportunity to evolve its virulence mechanisms in order to thrive in the harsh conditions imposed by the immune system and eventually allowing its transmission between hosts. In light of this ancient history between host and pathogen, a greater understanding of Mtb and its interactions with the host will be required to develop more efficient anti-TB drugs and vaccines. In this work we have focused on the role of the Mtb protein Rv0101, a non-ribosomal peptide synthetase predicted to be involved in lipid metabolism and cell wall biogenesis, during infection. We found that mice infected with a Mtb mutant deficient for Rv0101 have a transient lower lung bacterial burden during the early stages of infection. Additionally, in mice infected with this strain the dissemination of the bacterium to the spleen was delayed and remained lower up to 90 days post-infection. These differences were accompanied by a diminished recruitment of activated CD4+ T cells, inflammatory monocytes and an overall lower immunopathology. Furthermore, mice with severely compromised or absent adaptive immune response were able to survive infection with this mutant strain at least twice as long as animals infected with the complemented strain. In summary, we have shown that Rv0101 is a virulence factor required by Mtb to optimally overcome the innate immune response of the host, in addition to being a potent inducer of immunopathology. Characterizing the role of key Mtb molecules in infection is urgently needed to understand how the pathogen overcomes and modulates the host immune response to allow for its persistence and transmission. In turn, this knowledge may provide good drug targets and a better rational for vaccine design.

RESUMO

O *Mycobacterium tuberculosis* (Mtb), agente etiológico da tuberculose (TB), é um agente patogénico altamente complexo sendo estimado que tenha levado a mais mortes que qualquer outro agente infeccioso ao longo da existência humana. Apesar de esforços globais para erradicar a TB, ela continua a liderar como uma das causas de morte por doença infecciosa, sendo ultrapassada apenas pelo vírus da imunodeficiência humana (HIV). Apesar de medidas de saúde pública terem diminuído o fardo da TB, a realidade é que nas ultimas décadas pouco mudou em termos da terapia anti-TB e vacinação. Como um patógeno intracelular obrigatório, o Mtb co-evoluiu com o seu hospedeiro humano durante mais de 70 mil anos. Esta janela temporal conferiu ao Mtb amplas oportunidades para evoluir os seus mecanismos de virulência de forma a prosperar no ambiente hostil imposto pelo sistema imune inato, eventualmente permitindo a sua transmissão entre hospedeiros. À luz deste história milenar entre hospedeiro e patógeno, uma maior compreensão do Mtb e das suas interacções com o hospedeiro serão necessárias ao desenvolvimento de antibióticos e vacinas mais eficientes. Neste trabalho focámo-nos no papel durante a infecção do Rv0101 do Mtb, uma sintetase peptídica não ribossomal previsivelmente envolvida em metabolismo lipídico e na biogénese da parede celular. Mostramos que ratinhos infectados com um mutante deficiente para o Rv0101 apresentam uma carga bacteriana temporariamente inferior durante o estágio inicial da infecção. Além disso, esses mesmos ratinhos apresentaram um aparecimento tardio da bactéria no baço e controlaram-na melhor pelo menos até ao dia 90 após a infecção. Estas diferenças foram acompanhadas por um recrutamento diminuído de células T CD4+, monócitos inflamatórios e em geral uma menor imunopatologia. Adicionalmente, ratinhos sem sistema imune adaptativo, ou com o mesmo severamente comprometido, infectados com com esta estirpe mutante conseguiram sobreviver pelo menos o dobro do tempo que aqueles infectados com a estirpe complementada. Resumidamente, mostramos que o Rv0101 é um factor de virulência do Mtb, necessário para uma óptima superação da resposta imune inata do hospedeiro, sendo também capaz de induzir diferenças imunopatológicas duradouras. A caracterização do papel de moléculas do Mtb durante a infecção será necessário para compreender como o patógeno supera e modula a resposta imunitária do hospedeiro, permitindo a sua persistência e transmissão. Por sua vez, este conhecimento pode providenciar bons alvos para novas drogas e assistir no desenho de novas vacinas.

TABLE OF CONTENTS

ABSTRACT vii

RESUMO ix

FIGURE INDEX xiii

LIST OF ABBREVIATIONS xv

INTRODUCTION 1

1. Epidemiology 3
2. Early events in the immune response to Mtb 4
    - 2.1. Transmission 4
    - 2.2. Innate immune response 4
    - 2.2.1. Recognition 4
    - 2.2.2. Inflammatory mediators 4
    - 2.2.2.1. IL-12p40 - homodimers and heterodimers 5
    - 2.2.2.2. IL-6 6
    - 2.2.2.3. TNF-α 6
    - 2.2.2.4 The IL-1β – Eicosanoid – Type-1 IFN network 6
    - 2.2.2.5. Chemokines 8
    - 2.3. Adaptive immune response 9
3. Host-pathogen interactions 12
    - 3.1. The cell wall of Mtb and its impact in host-pathogen interactions 12
    - 3.1.1. TDM 14
    - 3.1.2. PDIMs 14
    - 3.1.3. SLs 15
    - 3.1.4. Other cell wall lipids 15
4. The role of Rv0101 in Mtb virulence 16

AIMS 17

METHODS 21

1. Bacteria and Infection 23
2. Animals 23
3. Differentiation and Infection of Bone Marrow-Derived Macrophages (BMDM) and Peritoneal Macrophages 23
4. Sample Collection and Preparation of Single Cell Suspensions 24

5. Survival 25
6. Bacterial Burden Determination 25
7. Histology 25
8. Flow Cytometry 25
9. Mtb growth curves 26
10. Cytokine concentration by Enzyme-Linked Immunosorbent Assay (ELISA) 27
11. RNA extraction and quantification 27
12. Reverse transcriptase polymerase chain reaction (RT-PCR) 27
13. Quantitative Real-Time PCR (qRT-PCR) 27
14. Statistical Analysis 28

RESULTS 29
1. Initial considerations 31
2. *In vivo* infection 32
2.1. Nrp is required for optimal establishment of infection 32
2.2. Nrp induces lung immunopathology 33
2.3. Immune response characterization 35
2.3.1. Nrp modulates the cellular immune response 36
2.3.2. Cytokine and chemokine expression is modulated by nrp 40
2.3.3. Nrp is required for full virulence in mouse models of deficient adaptive immunity 43
2.3.4. Innate immune deficiencies 46
2.3.4.1. Nrp-dependent virulence is not mediated by TLR-2 or TLR-4 activation 46
2.3.4.2. Nrp-dependent virulence is not mediated by the eicosanoid pathway 47
3. *in vitro* studies 48

DISCUSSION AND FUTURE PERSPECTIVES 53

REFERENCES 63

FIGURE INDEX

Figure 1	The balanced IL-1 β – eicosanoid – type-I IFN network.	Page 8
Figure 2	The cellular immune response to Mtb.	Page 11
Figure 3	Schematic representation of the cell envelope of Mtb.	Page 13
Figure 4	Cytometry analysis.	Page 26
Figure 5	nrp-complemented and Δnrp-mutant strains growth kinetics in liquid media.	Page 31
Figure 6	Animals infected with the Δnrp-mutant or the nrp-complemented strain presented different bacterial burdens over time in the lungs and spleen.	Page 32
Figure 7	Animals infected with the Δnrp-mutant or the nrp-complemented strain presented different immunopathology in the lungs.	Page 33
Figure 8	Characterization of H&E preparations from the lungs of animals infected with the Δnrp-mutant or the nrp-complemented strain revealed differences in immunopathology.	Page 34
Figure 9	The Δnrp-mutant and nrp-complemented strain induced different myeloid cell recruitment in the lungs of WT mice.	Page 37
Figure 10	Total number of alveolar macrophages was independent of infecting strain.	Page 38
Figure 11	The Δnrp-mutant and nrp-complemented strains present different CD4+ T cell features in the lungs of WT mice.	Page 39
Figure 12	The Δnrp-mutant and nrp-complemented strain induced differential cytokine/chemokine expression in the lungs of WT mice.	Page 42
Figure 13	The Δnrp-mutant presented reduced virulence in RAG-2 deficient mice.	Page 44
Figure 14	The Δnrp-mutant presented reduced virulence in IFN- γ deficient mice.	Page 45
Figure 15	nrp does not appear to modulate the recognition of Mtb by immune cells through TLR-2 and TLR-4.	Page 46

Figure 16	Shifting the eicosanoid pathway towards PGE2 production did not seem to impact control of the Δnrp-mutant.	Page 47
Figure 17	The eicosanoid pathway was not modulated by nrp.	Page 48
Figure 18	nrp was required for optimal Mtb growth inside macrophages but did not protect against IFN-γ dependent mechanisms.	Page 49
Figure 19	The Δnrp-mutant induced higher nitric oxide production than nrp-complemented Mtb.	Page 50
Figure 20	The Δnrp-mutant induced higher production of TNF-α, but not IL-1β or IL-10, than the nrp-complemented Mtb.	Page 51
Figure 21	Summary of the main findings and questions resulting of this thesis.	Page 62

LIST OF ABBREVIATIONS

AMP	Antimicrobial peptide
AIDS	Acquired immune deficiency syndrome
ALOX	Arachidonate lypoxigenase
AMPh	Adenosine monophosphate
ANOVA	Analysis of variance
APC	Antigen-presenting cell
BCG	Bacillus Calmette-Guérin
BDL	Below detection level
BMDM	Bone marrow-derived macrophages
CCL	C-C chemokine ligand
CR	Complement receptor
cDNA	Complementary DNA
CCR	C-C chemokine receptor
CFU	Colony-forming unit
CLR	C-type lectin receptor
DCs	Dendritic cells
ELISA	Enzyme-Linked Immunosorbent Assay
FBS	Fetal bovine serum
GMM	Glucose monomycolate
H&E	Hematoxylin-eosin
HIV	Human immunodeficiency virus
IFN	Interferon
IL	Interleukin

LAM	Lipoarabinomannans
LCCM	L929-cell-conditioned medium
LM	Lipomannans
LOS	Lipooligosaccharides
LTB4	Leukotriene B4
LXA4	Lipoxin A4
MDR	Multidrug resistant
MOI	Multiplicity of infection
MHC	Major histocompatibility complex
MMP	Matrix metalloproteinase
mRNA	Messenger RNA
Mtb	Mycobacterium tuberculosis
MyD88	Myeloid differentiation primary-response protein 88
NOD2	Nucleotide-binding oligomerization domain-containing protein 2
NOS2	Nitric oxide synthase 2
Nrp	Non-ribosomal peptide synthetase
OADC	Oleic acid/albumin/dextrose/catalase
PAMP	Pathogen-associated molecular patterns
PB	Proskauer Beck
PBS	Phosphate-buffered saline
PDIM	Phthiocerol dimycocerosate
PGE2	Prostaglandin E2
PIM	Phosphatidylinositolmannoside
PPE	Proline-Proline-Glutamic acid
PRR	Pattern recognition receptors
RNS	Reactive nitrogen species

RORγt	Retinoic acid receptor-related orphan receptor- γ t
RAG	Recombination activating gene
ROS	Reactive oxygen species
SL	Sulfolipids
SR	Scavenger receptor
TB	Tuberculosis
TGF-β	Transforming growth factor-β
TRIF	TIR-domain-containing adapter-inducing interferon- β
TDM	Trehalose dimycolate
Th	T helper
TLR	Toll-like receptor
TNF	Tumor necrosis factor
WHO	World Health Organization
WT	Wild-type

INTRODUCTION

1. Epidemiology

Tuberculosis (TB) is an infectious disease caused by *Mycobacterium tuberculosis* (Mtb). As a predominantly lung disease, some of its main clinical features include sputum producing chronic cough, appetite and weight loss, night sweats, fever, hemoptysis and ultimately mortal respiratory failure in case treatment fails[1]. To the furthest extent of our knowledge, TB has killed more people than any other infectious disease, and it is estimated to have killed more than smallpox, malaria, plague, influenza, cholera and acquired immune deficiency syndrome (AIDS) combined in the past two hundred years[2]. Despite major global efforts towards prevention and treatment, TB remains one of the leading causes of death due to infectious disease, second only to human immunodeficiency virus (HIV)[3]. In is estimated that 2 billion people are affected by a latent form of this disease and in 2013 alone 9 million new cases of active TB and 1.5 million deaths were registered[3]. Although the numbers of new TB cases and its death toll are still a matter of grievous concern, they are in drastic contrast to the reality observed during the first half of the twentieth century[2,3]. Since the beginning of the twenty first century, there has been an average 1.5% decrease of TB incidence per year, accompanied by an overall decrease of disease prevalence and mortality, and a stabilization of TB incidence among HIV-positive patients[3]. Even though these data are overall positive, a drastic decrease in the drop of TB incidence rate was observed between 2012 and 2013, registering a drop of 0.6%, less than half of the average since 2000[2,3]. To reach the milestone of less than a TB case per million individuals set by the World Health Organization (WHO) for 2050, numerous roadblocks will have to be overcome. Among these, the most notorious are the absence of an efficient vaccine, the lack of fast and reliable diagnostic tools and the requirement for more efficient anti-mycobacterial drugs. Furthermore, the large number of TB/HIV co-infections and the increased incidence of infections with multidrug resistant (MDR) Mtb strains further prevent the success of this milestone. Indeed, the current strategy to stave off TB is based on public health measures, a 50 years old multidrug regimen for at least six months and the inconsistent protection of the Bacillus Calmette-Guérin (BCG) vaccine[3,4]. It is clear that a greater understanding regarding the mechanisms underlying the success Mtb as a pathogen is required to develop more efficient vaccines and drugs. In the past few decades, efforts have been made to close this gap of knowledge, both regarding the immune system, the pathogen and their interactions, a topic that will be further developed in this thesis.

2. Early events in the immune response to Mtb

2.1. Transmission

It is thought that transmission of Mtb occurs when an infected individual with an advanced form of TB, characterized by high bacterial burden coughs and disrupted lesions with access to the airways, coughs and releases small bacteria-containing droplets into the atmosphere, which will subsequently be inhaled by individuals in close proximity[5]. Although transmission models of TB have not yet been fully established, it is though that mainly the smaller infectious droplets, containing fewer bacteria, will make it past the upper respiratory track, and into the relatively sterile environment of the distal alveoli[6–8].

2.2. Innate immune response

2.2.1. Recognition

Once in the distal alveoli, recognition and phagocytosis of the bacteria occurs mainly by alveolar macrophages, but also by dendritic cells (DCs), monocytes, neutrophils and even by epithelial cells [9–14]. Several receptors expressed in phagocytic cells are known to bind pathogen-associated molecular patterns (PAMPs) present in Mtb. These receptors include toll-like receptors (TLRs), nucleotide-binding oligomerization domain-containing protein 2 (NOD2), C-type lectin receptors (CLRs), scavenger receptors (SRs) and complement receptors (CRs)[15,16]. Although *in vitro* studies have revealed a specific role for many of these receptors in response to Mtb, most *in vivo* works using animals deficient for a single receptor revealed only a minor or no phenotype[16]. These studies suggest that recognition of Mtb by innate immune cells is a complex event requiring multiple receptors, with some of them probably sharing some degree of redundancy[16].

2.2.2. Inflammatory mediators

Upon recognition and internalization, a vast array of inflammatory mediators is released to the vicinity of the infected cell in response to stimulation of pattern-recognition receptors (PRRs) by Mtb PAMPs[17,18]. These mediators include the interleukin (IL)- 12 subunit IL-12p40, tumor necrosis factor α (TNF-α), IL-6 and IL-1β, eicosanoids, type-I interferons (IFN) and chemokines[18]. Together these molecules shape the immune response to Mtb.

2.2.2.1. IL-12p40 - homodimers and heterodimers

Overall, the relevance of IL-12p40 derived cytokines is highlighted by the fact that humans with mutations on the IL-12β1 receptor present higher susceptibility to TB resulting in increased incidence, severity and disease dissemination[19–25].

IL-12p40 dimerizes either with another IL-12p40 molecule, IL-12p35 or IL23-p19, forming IL-12p80, IL-12 (also known as IL-12p70) and IL-23, respectively[18,26]. IL-12p80 is readily formed after infection and is essential to induce a migratory phenotype in DCs, allowing them to travel to the lymph node where naïve T cells will be activated[5,14,18,27], thus triggering and adaptive immune response. This IL-12p80 dependent mechanism is believed to be enhanced through the expression of a splice variant of the IL-12β1 receptor (which binds to IL-12p40) by DCs early after infection[28]. Although IL-12p80 is important in the early events leading to the adaptive immune response, it is unable to trigger the production of IFN-γ, a critical cytokine required for the control of Mtb[29].

IL-12p40 also dimerizes with IL-12p35. Unlike IL-12p40, IL-12p35 is not significantly expressed in the early stages after Mtb infection[29]. Accordingly, the critical role of IL-12p70 does not involve the initial triggering of an adaptive immune response to Mtb, as is the case of IL-12p80[19,30]. Instead, IL-12p70 is essential in the induction and maintenance of IFN-γ-producing cells, which are protective in later stages of infection[19,30]. Thus, IL-12p70 is essential for long lasting protection against Mtb, as mice lacking this cytokine are unable to control bacterial proliferation[19,29].

The dimerization of IL-12p40 with IL-23p19 leads to the formation of IL-23 which, in contrast to IL-12p70, is not essential to control Mtb infection[14]. Indeed, mice lacking IL-23p19 infected by a low-dose aerosol are equally able to control Mtb as WT mice[30]. However, IL-23 is required for optimal differentiation of an IL-17-producing adaptive immune response[30]. The relevance of this type of adaptive immune response is discussed later in this work. Furthermore, IL-23 is known to share some functions with IL-12p70. Specifically, IL-12p35 deficient mice are able to generate an IFN-γ-producing adaptive immune response through an IL-23p19 dependent mechanism[30]. However, this mechanism does not fully compensate the absence of IL-12p70, as the adaptive immune response triggered is not sufficient to control Mtb[30].

2.2.2.2. IL-6

Although IL-6 is rapidly produced by phagocytes after Mtb challenge, its relevance in the context of infection is still a matter of debate[18]. It is currently known that IL-6 is required for the induction of an optimal T cell response[31], even though after low dose aerosol infection IL-6 deficient mice are able to control Mtb with only a slight increase in lung bacterial burden[32]. On the other hand, when these mice are exposed to a high-dose aerosol they rapidly succumb to infection[33], clearly pointing for a role for this cytokine as a necessary response factor against high-burden challenges.

2.2.2.3. TNF-α

Unlike IL-6, it is well established that TNF-α is essential to control Mtb, as TNF-α deficient mice are unable to control the growth of Mtb and quickly succumb to infection[34–36]. The importance of this cytokine is further emphasized by human studies. Indeed, rheumatoid arthritis and inflammatory bowel disease patients undergoing the standard anti-TNF therapy have an increased chance to reactivate a latent case of TB[37–39]. TNF-α exerts its main function in controlling Mtb by activating microbicidal mechanisms in macrophages, thus allowing for the elimination of Mtb[10]. In addition to this critical function during the earlier stages of TB, TNF-α plays a role in the formation of the granuloma and is essential to maintain its structural integrity during infection, allowing a better control of Mtb during the chronic stage of infection[40,41].

2.2.2.4 The IL-1β – Eicosanoid – Type-1 IFN network

The exact role of IL-1β in TB has not yet been fully characterized, but it is clear that mice lacking this cytokine or its receptor are highly susceptible to Mtb, and succumb shortly after infection[42,43]. Furthermore, this cytokine requires a tight regulation, as its overproduction leads to extreme immunopathological features associated with poor survival[44]. Even though IL-1β exerts a protective role against Mtb, it does so independently of TNF-α, IFN-γ, nitric oxide synthase 2 (NOS2) and IL-12p40[44,45]. Indeed, the levels of these molecules were not diminished in mice deficient for IL-1β signaling when compared to WT animals[44,45]. More recently however, the role of IL-1β has been partially attributed to the regulation of the eicosanoid pathway[46].

The eicosanoid pathway has only recently been implicated in the immune response to Mtb[47,48]. The eicosanoids are immunomodulatory lipids derived from arachidonic acid and are divided into 3 distinct classes: prostaglandins (PGs), leukotrienes (LTs) and lipoxins (LXs)[49]. All these classes of eicosanoids are produced by infected macrophages and it has been proposed that the ratio between each individual class may significantly impact the outcome of infection[14]. Specifically, PGE2 is known to induce apoptosis of infected cells leading to phagocytosis of apoptotic cells by phagocytes in their vicinity (efferocytosis), a mechanism associated with protection against Mtb[47,50]. Indeed, arachidonate 5-lypoxigenase (ALOX5) deficient mice, which are unable to produce LTB4 and LXA4 thus shifting the metabolic pathway towards PGE2 production, are more resistant to Mtb[51]. In contrast, LXA4 induces a necrotic phenotype in infected cells, which favors bacterial proliferation and infection of bystander cells, thus enabling the formation of new infectious foci[14,47,50]. The extent of the role of eicosanoids is not yet fully understood, but human studies highlight their relevance in TB. Specifically, polymorphisms in *Alox5* and *Lta4h* (involved in LTA4 synthesis) increase susceptibility to TB[52,53]. From an immunological standpoint, PGE2 production has been shown to be induced by IL-1β, and in addition to its direct effects in the control of Mtb, it also plays a role in regulating the crosstalk between IL-1β and type-I IFN[46,54,55].

Type-I IFNs comprise IFN-α and IFN-β and have been associated with detrimental effects to the host during Mtb infection, both in humans and in the mouse model. Specifically, high severity of active TB correlates with high levels of circulating type-I IFNs and high levels of expression of genes induced by these cytokines[46,56]. Accordingly, mice deficient in the receptor for these cytokines show increased survival and lower bacterial burdens upon Mtb infection[57,58]. It has been suggested that type-I IFNs exert their detrimental role in TB by downregulating the production of IL-1β and IL-12, partially due to an increase in IL-10 and IL-1β antagonist production[45,54,55,59]. A schematic of the crosstalk between these cytokines is proposed in Figure 1.

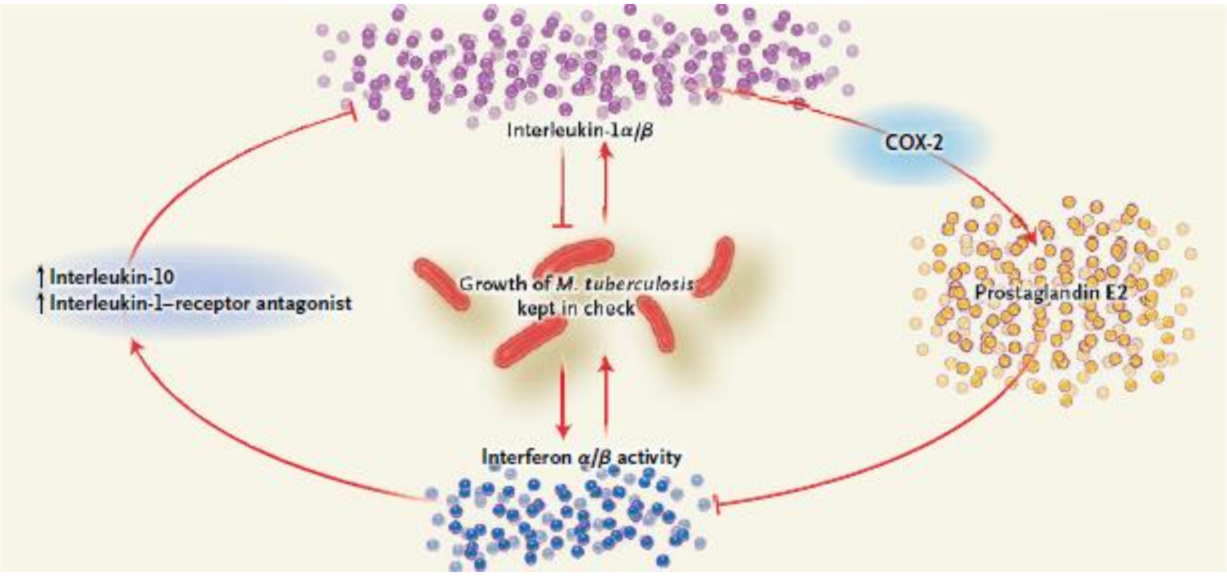

Figure 1: The balanced IL-1β – eicosanoid – type-I IFN network. Mtb induces IL-1α/β and type-I IFN production. IL-1β activates cyclooxygenase-2 (COX-2) resulting in PGE2 production. PGE2 inhibits type-I IFN activity, favoring control of Mtb. Type-I IFN induces IL-10 and IL-1R antagonist, blocking IL-1β activity and favoring Mtb growth. Originally from Jon S. Friedland, Clinical Implications of Basic Research, The New England Journal of Medicine, 2014.

The relevance of the immune network formed by IL-1β, eicosanoids and type-I IFNs has just begun to be explored, but it already presents itself as a good target for anti-TB therapy, with the possibility to be used in a patient-specific manner[54,55].

2.2.2.5. Chemokines

In addition to cytokines, chemokines play a major role in building the inflammatory environment encountered in TB. These chemokines are predominantly composed by two distinct classes, defined by the presence of a C-C or C-X-C motif and a single receptor may be able to bind multiple chemokines[60]. This family of proteins is responsible for orchestrating the recruitment of leukocytes to the site of infection and subsequent migration to different organs[60]. In the mouse model, there are at least 34 chemokines reported to be differential expressed throughout Mtb infection[60], attesting the complexity of the cell-recruitment dynamics encountered during infection. Resorting to gene deficient mice, a vast effort has been placed towards characterizing the role of individual chemokines and their receptors in the context of Mtb infection. Few of these studies have reported differences regarding bacterial burden, and when these differences were reported they are predominantly in mice deficient for a chemokine receptor[60]. Indeed, only few studies reported a role for individual chemokines, suggesting a redundant role for these molecules[60–63]. Specifically, these studies have reported that mice deficient in C-C chemokine ligand 2 (CCL2), a CCR2 ligand, have a transient increase in lung bacterial burden after low-dose aerosol infection, accompanied by a decreased macrophage influx and accumulation of protective IFN-γ CD4+ T cells[64]. These findings are in line with the increased risk of developing TB presented by humans with a *Ccl2* polymorphism[65]. A similar phenotype was observed in mice deficient in CCL5 (CCR1/CCR5 ligand), although in this case the transiently increased lung bacterial burden was associated with a delayed recruitment of CD11c+ myeloid cells and T cells[66]. Other studies have shown that mice deficient for CCR7 or its known ligands (CCL19/CCL21) have an impaired DC migration to the lymph node, and are consequently impaired in T cell induction, translating into a diminished control of Mtb[67–70]. Interestingly, the action of chemokines is not restricted to cell-migration between organs, as they also play a role in the location of immune cells within the inflammatory lesion. Specifically, mice deficient in CXCL13 (CXCR5 ligand) have been shown to be more susceptible to Mtb, not due to an overall change in the number of a specific cell type, but instead due to the location of T cells within the granuloma[69]. In this case, in the absence of CXCL13, T cells were unable to locate in close proximity to infected macrophages, thus leading to insufficient macrophage activation and subsequent Mtb growth[69].

Taken together, these studies point for a complex role of chemokines during infection, controlling temporal and spatial features of the formation and action of both innate and adaptive immunity.

2.3. Adaptive immune response

The activation of the innate immune response is crucial for the establishment of an adaptive immune response. It is known that 8-10 days after infection, antigen-presenting cells (APCs) carrying Mtb or Mtb molecules, mainly DCs, arrive at the lymph nodes[14]. Once in the lymph node, these cells will present Mtb molecules to naïve T cells, driving their differentiation and proliferation, and up to 5 days later these Mtb-specific T cells reach the site of infection[5,14]. It has been extensively described in humans and mice that adaptive immune responses are absolutely required to control Mtb. Specifically, HIV patients with low CD4+ T cell counts quickly succumb to Mtb infection if not rapidly treated[4,71,72]. A similar outcome is observed in recombination activating gene (RAG) deficient mice, which are unable to produce B and T lymphocytes and quickly succumb to Mtb shortly after infection[73].

There are two main CD4+ adaptive immune responses involved in TB, the T helper 1 (Th1) and Th17 responses. These responses are generated when APCs present Mtb peptides in the context of a major histocompatibility complex class 2 (MHC-II) to naïve CD4+ T cells in the presence of a specific cytokine milieu. For a CD4+ naïve T cell to acquire a Th1 phenotype it requires the expression of the transcription factor T-bet and IL-12 and IFN-γ as polarizing cytokines[26,29,74,75]. One the other hand, for optimal Th17 polarization expression of the transcription factor retinoic acid receptor-related orphan receptor-γt (RORγt) is required, as well as the presence of IL-6, transforming growth factor-β (TGF-β), IL-1β and IL-23[14,74,75].

The currently accepted paradigm is that a Th1 cell response must be induced for the host to control an otherwise lethal Mtb infection[10,11,76]. The Th1 cell subset is mainly characterized by the production of IFN-γ, which activates macrophages leading to the production of reactive nitrogen and oxygen species (RNS and ROS) [10,11,14,77–80]. In the mouse model, the onset of a Th1 cell adaptive immune response leads to the stabilization of bacterial burden[10,11,14]. Indeed, mice deficient for IFN-γ, NOS2 or MHC-II are unable to control bacterial growth and rapidly succumb to infection[77,81,82]. Although the Th1 cell subset is clearly essential for the host's protection, it is not able to sterilize the infected, even after boosting this response with the currently available vaccine.

To a lesser extent, the Th17 cell subset also plays a role in the immune response to Mtb. This subset secretes mainly IL-17 which is known to modulate granuloma formation and is required for BCG vaccine-dependent accelerated recruitment of IFN-γ producing T cells to the site of infection[83,84]. However, it has been shown that repeated BCG exposure of Mtb-infected mice leads to increased Th17 cell responses accompanied by neutrophil/granulocyte recruitment and consequently increased immunopathology due to enhanced neutrophilia[85]. Thus, although the induction of a Th17 response is largely benign in the context of TB, a tight regulation is required to avoid immunopathological consequences to the host[83].

During the immune response in TB, both Th1 and Th17 cell subsets are active and it is likely that a fine balance between them is required for a better outcome of TB. In this regard, it is known that Th1 cells are able to act as a negative regulator of the Th17 response by limiting neutrophil recruitment and downregulating IL-17 expression[73], thus limiting excessive immunopathology. On the other hand, IL-17 is able to anticipate the recruitment of Th1 cells, thus improving resistance to infection[86]. The mechanisms through which the host and Mtb regulate these different subsets of Th cells are not fully understood. It is possible that the key to a more efficient vaccine lies in finding the right balance between Th1 and Th17 cells.

The immune response in TB is a vast field of study, and although numerous works have helped to shed light on the matter, we are still unaware of the full spectrum of the mechanisms that govern this response and most importantly if there is an immune response capable of completely eliminating the pathogen. A simplified version of current knowledge regarding the cellular immune response to Mtb after low-dose aerosol infection is depicted in Figure 2.

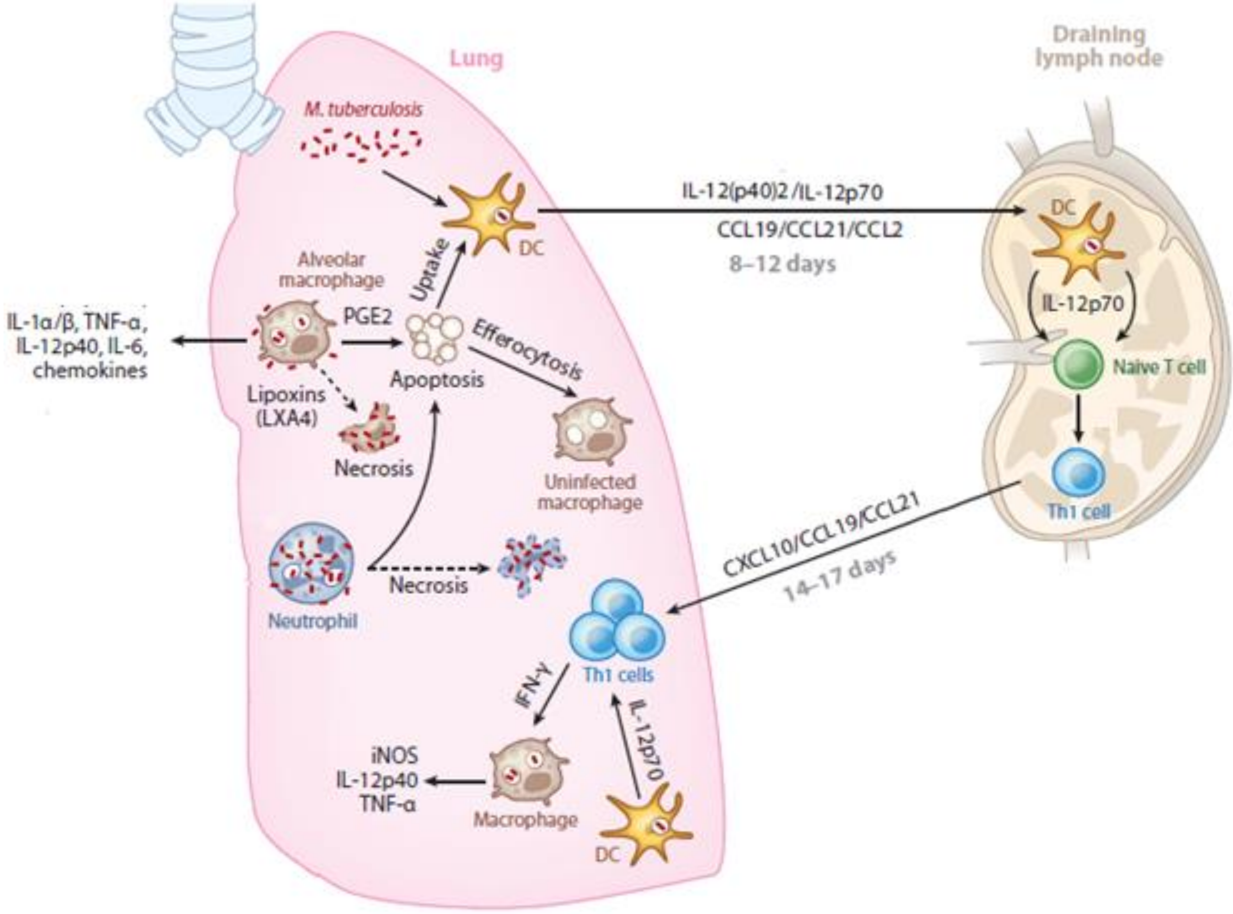
Lung
Draining lymph node
M. tuberculosis
DC
IL-12(p40)2/IL-12p70
CCL19/CCL21/CCL2
8–12 days
DC
IL-12p70
Naive T cell
Th1 cell
Alveolar macrophage
Uptake
IL-1α/β, TNF-α, IL-12p40, IL-6, chemokines
PGE2
Apoptosis
Efferocytosis
Lipoxins (LXA4)
Necrosis
Uninfected macrophage
CXCL10/CCL19/CCL21
14–17 days
Neutrophil
Necrosis
Th1 cells
IFN-γ
IL-12p70
iNOS
IL-12p40
TNF-α
Macrophage
DC

Figure 2: The cellular immune response to Mtb. After aerosol infection, Mtb can be phagocytosed by DCs, alveolar macrophages and neutrophils. Alveolar macrophages secrete inflammatory mediators including IL-1, IL-12p40, IL-6 and chemokines and together with neutrophils may die an apoptotic or necrotic cell death. DCs migrate to the draining lymph-node 8-12 days after infection, under the influence of CCL2, CCL19, CCL21, IL-12p80 (IL-12(p40)2) and IL-12P70. Th1 cells are generated upon antigen presentation in the presence of IL-12p70. Th1 cells migrate to the lung 14-17 days after infection under the influence of CCL2, CCL19 and CCL21. Upon arrival to the lung, Th1 cells required IL-12p70 for maintenance and activate macrophages by secreting IFN-γ. These macrophages increase in microbicidal activity by upregulating NOS2 (iNOS), TNF-α and IL-12p40 production. Adapted from Anne O'Garra, *et al.*, The Immune Response in Tuberculosis, Annual Reviews of Immunology, 2013.

3. Host-pathogen interactions

The events that take place in the immune response during TB are the result of a complex interaction between the host and Mtb. A great portion of the work performed on deciphering this immune response has focused on characterizing host factors, often disregarding how pathogen factors modulate this response. Indeed, our knowledge on how Mtb is able to subvert and thrive under the seemingly unfavorable conditions found within the host is still unclear. To fully understand the intricate relationship between Mtb and humans, the only host known for Mtb, we must consider that both have been coevolving since the appearance of anatomically modern humans about 70 000 years ago[87]. This time frame has given both host and pathogen ample opportunity to fine tune their defense and virulence mechanisms, respectively, to one another[87]. Indeed, the fact that TB presents a wide range of outcomes, ranging from clearance after infection, to establishment of subclinical latent disease and ultimately to active disease attests to the complexity of TB[1,4,14]. Remarkably, for extended periods of time in active TB, the balance between a protective and detrimental immune response allows the host to remain ambulatory, thus increasing the opportunity for Mtb to be transmitted[5]. These different outcomes may be largely defined by the result of the initial interaction between Mtb and innate immune cells[1]. Accordingly, it has been shown that different strains of Mtb induce different inflammatory profiles after infection of these cell types[88–91].

3.1. The cell wall of Mtb and its impact in host-pathogen interactions

The initial interactions between Mtb and the host are predominantly dependent of recognition of antigens present of the cell wall of Mtb by the PRRs on innate immune cells. This cell wall is an extremely complex structure, composed by 4 distinct layers: the innermost polysaccharide layer composed by peptidoglycans and arabinogalactan; the inner mycomembrane composed of long chain mycolic acids covalently attached to the innermost proteins; the outer mycomembrane composed many non-covalently lipids, including phthiocerol dimycocerosates (PDIMs); trehalose dimycolate (TDM); sulfolipids (SLs); phosphatidylinositolmannosides (PIMs) modified into lipomannans (LM) and lipoarabinomannans (LAM); glucose monomycolate (GMM); lipooligosaccharides (LOS); and the outermost capsular layer containing poorly characterized glycans, lipids and proteins[92,93]. A simplified schematic representation of the cell envelope of Mtb is depicted below in Figure 3.

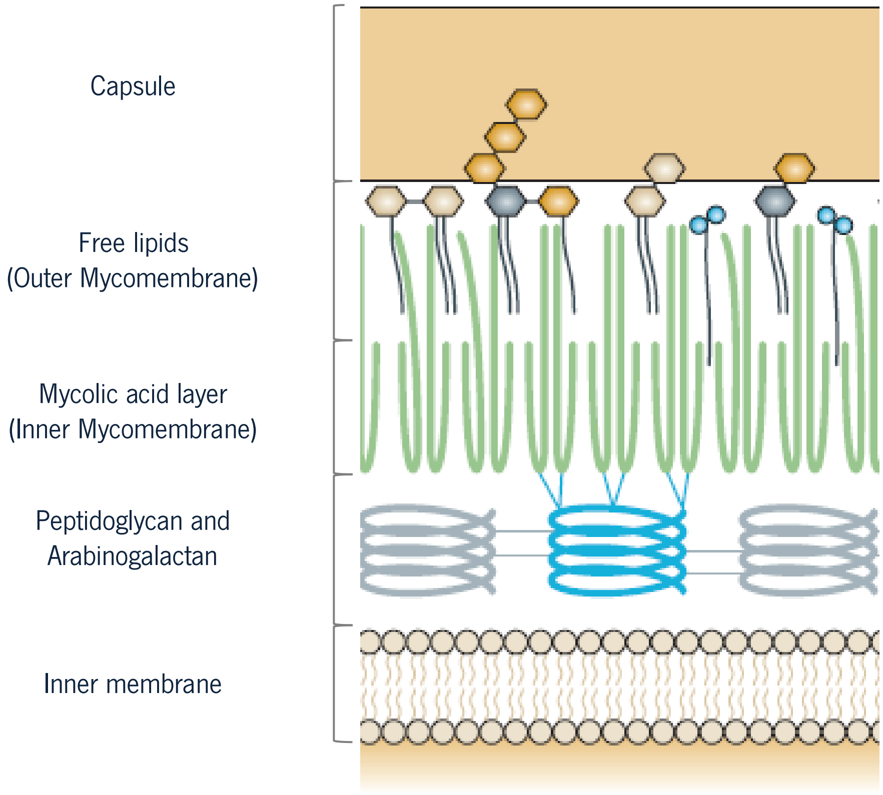

Figure 3: Schematic representation of the cell envelope of Mtb. The cell wall is mainly composed by a large complex that contains three different covalently linked structures (peptidoglycan (grey), arabinogalactan (blue) and mycolic acids (green)). The outer mycomembrane contains various free lipids non-covalently linked to mycolic acids. These free lipids include TDM, PDIMs, SLs, LOS, GMMs, PIMs and its glycoconjugates. The capsule contains poorly characterized glycans, lipids and proteins. Adapted from Abdallah M. Abdallah, *et al.*, Type-VII secretion – mycobacteria show the way, Nature Reviews Microbiology, 2007[94].

These lipid components of the outer mycomembrane and capsular layer are thought to be in direct contact with the host's cells and therefore their study is important to understand how their recognition modulates the immune response[16].

As a result of the availability of the Mtb genome, and upon the development of efficient techniques to genetically manipulate this pathogen[95,96], the employment of gene-deficient Mtb has allowed us to assess the role of specific Mtb molecules during infection. Particularly, this has allowed us to gain insight on the role of the relevance the Mtb cell wall lipids in infection.

3.1.1. TDM

Among Mtb cell wall lipids, TDM is one of the most studied. This lipid is recognized by Mincle (a C-type lectin) and has been consistently associated as a virulence factor o Mtb[15]. Specifically, WT mice infected with a Mtb strain deficient for an enzyme responsible for adding distal-oxygen groups to mycolates presented increased survival when compared to mice infected with the WT strain[97]. In subsequent studies, this phenotype was attributed to an increased induction of IL-12p40 and TNF-α by the mutant strain[98–100]. Indeed, mice deficient for IL-12p40 presented the same survival time, regardless of the infecting Mtb strain[98].

3.1.2. PDIMs

PDIMs were first reported to be a virulence factor upon the observation that Mtb clinical isolates deficient for PDIMs were unable to induce a severe disease in the ginea pigs[101]. More recently, it has been reported that PDIM-deficient Mtb induces a hyper inflammatory profile in macrophages, putatively due to higher exposure of PAMPs[8]. Additional, studies have shown that PDIM-deficient Mtb has an impaired growth inside resting macrophages, although these studies reported opposing results regarding the role of PDIMs on phagosomal acidification[102,103]. Recently, work performed with *Mycobacterium marinum* in the zebrafish larvae model has elegantly shown that PDIMs exert a role in modulating the inflammatory environment towards a bacterium-permissive one[8]. Specifically, it was shown that by avoiding TLR detection, and without myeloid differentiation primary-response protein 88 (MyD88) activation, the bacterium is able to induce the recruitment of permissive macrophages to the site of infection[8]. These macrophages show a reduced NOS2 activation and are therefore a better environment for bacterial replication[8]. Unfortunately, this mechanism cannot fully explain the role of PDIMs in Mtb, as an independent study using the mouse model of infection was unable to rescue the phenotype observed with PDIM-deficient Mtb, even when infecting IFN-γ, NOS2, MyD88 and CCR2 deficient mice[104]. This particular study has shown that the lower bacterial burden, observed in PDIM-deficient Mtb infected animals, is due to an increased bacterial death, and not a deficit in replication, early during infection[104]. The question of whether PDIMs grant virulence by subverting any specific immune mechanism, or whether it does so by granting sheer cell wall integrity remains to be elucidated.

3.1.3. SLs

The role of SLs during infection has not yet been clearly defined, but they are suggested to relevant during infection since the cell wall composition of Mtb extracted from infected humans or animals is enriched in SLs when compared to the composition found in Mtb under culture conditions[105]. SLs are recognized by NOD2 and class A SRs[15,106], and as an anionic molecule it has been shown that SL-deficient Mtb has decreased susceptibility to LL-37, a human cationic antimicrobial peptide (AMP), by reducing Mtb-AMP interactions[107]. Despite this, no discernible phenotype has been observed between mice and murine macrophages infected with either WT or SL-deficient Mtb. Despite the fact that no differences regarding bacterial burden were observed, mice and guinea pigs infected with the SL-deficient Mtb presented a longer survival time than those infected with WT strain[108,109]. Interestingly, it has been reported that SLs are preferentially uptaken by neutrophils leading to high ROS production[110], a microbicidal mechanism that confers limited protection against Mtb. Whether SLs induce Mtb phagocytosis by neutrophils, a cell-type considered to be a permissive niche for mycobacterial growth[14], has not yet been assessed. One possible factor that may have hindered the attempt to define a clear role to SLs in TB is that the Mtb mutants employed so far were deficient exclusively for the SL-1 family. However, it has recently been proposed that the SL-2 family actually accounts for the highest quantity of SLs in Mtb[111], thus it is possible that by removing this predominant SL family more pronounced phenotypes may be discovered.

3.1.4. Other cell wall lipids

Although *in vitro* studies have provided compelling evidence that PIMs and its glycoconjugates are able to modulate recognition and phagosome maturation in macrophages[112–114], only limited *in vivo* work performed with Mtb mutants engineered for these structures has been published. Specifically, only one study using the zebrafish larvae model reported that a *Mycobacterium marinum* strain deficient for an enzyme required for LAM/LM branching, resulted in impaired growth of the bacterium when compared to the WT strain[115]. Hence, the role for these molecules during infection remains to be elucidated. Similarly, this Mtb-mutant strategy is yet to be employed for the study of GMMs and LOS.

It is now clear that Mtb has developed a cell wall capable of modulating the immune response of the host in its favor. The fact that these lipidic cell wall molecules are subject to modifications in saturation, chain length, cyclization among others with unpredictable effects[92,93], further affirms the complexity of this pathogen. The study of these host-pathogen interactions has just begun to scratch the surface of the intricacy beyond this timeless disease, but the employment of genetically engineered Mtb may prove a powerful tool to further advance this field of study.

4. The role of Rv0101 in Mtb virulence

The study of Mtb cell wall components has yielded valuable information on how host and pathogen interact, allowing for the choice of better targets for the future development of antimycobacterial drugs. However, there are still many unexplored Mtb molecules whose role during infection remains uncharacterized. Our knowledge on how the pathogen is able to thrive in the hostile conditions encountered inside the host could greatly benefit from the study of these molecules in the context of infection. Therefore, to advance this knowledge, we proposed to characterize a non-ribosomal peptide synthetase (nrp) encoded by Mtb, whose role during infection has not yet been defined.

Nrp is coded by Rv0101, and is part of a larger operon comprising other five genes: Rv0096, a member of the Proline-Proline-Glutamic acid (PPE) family; Rv0097, an oxidoreductase; Rv0098, a type III thioesterase; Rv0099, a fatty acid adenosine monophosphate (AMPh) ligase and Rv0100, which encodes an acyl carrier protein[116]. Nrp is predicted to interact with Rv0099 and Rv0101 to form a multimodal enzyme [117] and is an ubiquitous protein, present in cytosol, cell membrane and cell wall fractions of H37Rv [118]. Sequence analysis of the *nrp* gene predicts that this enzyme is involved in lipid metabolism [119]. The function of nrp in lipid metabolism together with its localization in the cell wall, are good indications that this enzyme takes part in cell wall synthesis.

Although so far no study has directly addressed the role of this enzyme, it has been mentioned multiple times in the literature as a potential Mtb virulence factor. Specifically, it was reported as a non-essential gene for *in vitro* growth by transposon mutagenesis, but was on the other hand required for growth in the spleen of C57BL/6J mice [119,120]. Interestingly, nrp was reported to be the most abundant Mtb protein in the lungs of infected guinea pigs by day 30 post infection, while being undetected at 90 days post infection [121], suggesting that Mtb regulates the expression of this protein throughout the course of infection. Overall these reports point for a strong role of nrp during infection.

Taking these data in consideration, in this present work we propose to characterize the relevance of nrp during infection, and how it impacts the interactions between Mtb and the host.

AIMS

Mtb is arguably the most successful pathogen known to mankind, with its existence spanning as long as that of mankind. To once and for all eradicate TB, a greater understanding of the fine mechanisms by which the pathogen is able to survive and thrive inside its human host is required. Many potentially pivotal Mtb virulence factors remain either unknown or uncharacterized, and their study could benefit greatly the development of new vaccines and anti-mycobacterial therapies.

The main goals of this thesis are to define the impact of nrp on:

The growth of Mtb under optimal culture conditions.

The interactions of Mtb with macrophages in an *in vitro* setting.

The course of Mtb infection in the mouse model.

The modulation of the innate and adaptive immune response of the host.

METHODS

1. Bacteria and Infection

Mtb Δnrp-mutant and nrp-complemented strains, were generated on a H37Rv background by Dr Apoorva Bhatt (School of Biosciences – University of Birmingham). Bacteria were grown in Middlebrook 7H9 liquid media (BD Biosciences) for 7–10 days and then sub-cultured in Proskauer Beck (PB) medium, supplemented with 0.05% Tween 80 and 2% glycerol, to the mid-log phase. Bacterial stocks were aliquoted and frozen at –80°C. To determine the concentration of Mtb aliquots, 6 frozen aliquots were serial diluted and plated in Middlebrook 7H11 (BD Biosciences) agar plates supplemented with 10% oleic acid/albumin/dextrose/catalase (OADC) and 0.5% glycerol. Viable bacteria were determined by counting colony-forming units (CFUs) after 19-21 days of incubation at 37°C.

Mice were infected via aerosol route using an inhalation exposure system (Glas-Col). Briefly, bacterial clumps were disrupted by forcing them through a 26G needle 6 times and diluted in water (Aqua B. Braun) to a concentration of $2x10^6$ CFU/mL. Mice were exposed to the infectious aerosol for 40 minutes, resulting in the delivery of 100-200 viable bacteria to the lungs. Assessment of initial bacterial burden was performed 3 days post infection by growing viable bacteria from the whole lung homogenate of 5 mice.

2. Animals

C57BL/6 mice were purchased from Charles River Laboratory (Barcelona, Spain). RAG-2 and IFN-γ (generated on a C57BL/6 background) deficient mice were generously provided by Dr. Margarida Correia-Neves (ICVS) and Dr. Susana Roque (ICVS), respectively. IL-10 (generated on a C57BL/6 background) deficient mice were a kind gift from Dr. Anne O'Garra (MRC-NIMR, London). ALOX-5, ALOX-15, TLR-2 and TLR-4 (generated on a C57BL/6 background) deficient mice were also purchased from Charles River Laboratory. All mice were kept and bred under the same conditions in the Life and Health Sciences Research Institute (ICVS) animal housing facilities, at the school of Health Sciences, University of Minho. All mouse protocols were performed according to the European Union Directive 2010/63/EU, and previously approved by *Direcção Geral de Alimentação e Veterinária*.

3. Differentiation and Infection of Bone Marrow-Derived Macrophages (BMDM) and Peritoneal Macrophages

Bone marrow cells were flushed from the tibiae and femurs of mice with complete Modified Eagle Medium (cDMEM, DMEM supplemented with 10% of heat-inactivated fetal bovine serum (FBS), 1% of HEPES 1M, 1% L-glutamine and 1% sodium pyruvate 100mM (all from GIBCO)). Bone marrow cells were counted and cultured in 8mL cDMEM supplemented with 20% L929-cell-conditioned medium (LCCM) at a concentration of 0.5 x 10^6 cells/mL in 8-cm diameter plastic petri dishes (Sterilin) for 7 days under 37°C and 5% CO_2 conditions. On day 4 of differentiation, 10mL of cDMEM supplemented with 20% LCCM were added to the cultures. At day 7, adherent cells were mechanically detached and seeded in 24-well plates (Nunc) at a concentration of $1x10^6$/well and incubated at 37°C. Cells were infected with Mtb at a multiplicity of infection (MOI) of 1:1 (bacteria/macrophage ratio) and incubated at 37°C with 5% CO_2. Four hours after infection, cells were washed 4 times with phosphate-buffered saline (PBS) (GIBCO) to remove extracellular bacteria. Washed cells were resuspended in 1mL of cDMEM and either incubated at 37°C for 48/96 hours in the presence or absence of 100 U/mL of IFN-γ or used to determine bacterial internalization. For that, 0.1% saponin (Sigma-Aldrich) in PBS was added to the wells and the cells were incubated at RT for 10 minutes to release intracellular bacteria. The number of viable bacteria was determined by plating 10-fold serial dilutions of the saponin treated cell suspensions in supplemented Middlebrook 7H11, as previously mentioned.

Peritoneal macrophages were obtained by intraperitoneally injecting 1 mL of thioglycollate in wild-type (WT) C57BL/6 mice. After 4 days, mice were euthanized and the peritoneum washed with PBS. The number of cells of the obtained peritoneal macrophage-enriched cell suspension was counted and processed for infection as described above for BMDM.

Supernatants from these cultures were used to determine nitric oxide concentration by the Griess method and cytokine concentration by ELISA.

4. Sample Collection and Preparation of Single Cell Suspensions

At selected time-points post-infection, mice were euthanized by CO_2 asphyxiation and the organs aseptically excised. Lungs were perfused with 10 mL PBS through the right ventricle of the heart to flush blood cells, sliced with 2 sterile scalpels and incubated at 37°C with collagenase IX (0.7mg/mL, Sigma-Aldrich) for 30 minutes. Single cell suspensions from the spleen and digested lung were obtained by homogenized by sieving them through a 40-µm-pore-size nylon cell strainer (BD Biosciences) with a syringe plunger. Lung and spleen cells were treated with erythrocyte lysis buffer (0.87% of NH4Cl solution and 5% of PBS in water) to lyse red blood cells and resuspended in cDMEM to use for bacterial burden determination, flow cytometry analysis and RNA extraction. Single cell suspensions were counted using a Countess® Automated Cell Counter (Life Technologies).

5. Survival

RAG-2 and IFN-γ deficient mice infected with Mtb weight was determined before infection and every 48 hours from day 30 post-infection onward. Mice were euthanized when they lost 20% weight or upon losing responsiveness to physical stimulation. Whenever possible, the lungs of moribund animals were harvested for histology and bacterial burden assessment.

6. Bacterial Burden Determination

To determine bacterial burdens, lung and spleen single cell suspensions were incubated with 0.1% saponin (Sigma-Aldrich) for 10 min to release intracellular bacteria. The number of CFUs was determined by plating 10-fold serial dilutions of saponin-treated cell suspensions in Middlebrook 7H11 agar plates supplemented as described above. BBL™ MGIT™ PANTA™ antibiotic mixture (BD Bioscience) was added to prevent contaminations of lung samples. Viable Mtb colonies were counted after 19-21 days of incubation at 37°C.

7. Histology

The right upper lobe of the lung was inflated with 5 mL of PBS containing 3.7% formaldehyde and kept for 1 week in this solution. Afterwards, these lobes were embedded in paraffin, sectioned in 2-3μm thickness slices, and stained with hematoxylin- eosin (H&E).

8. Flow Cytometry

For surface staining 1-2x10^6 cells were washed with FACS buffer (PBS containing 2% FBS and 0.01% azide) and stained for surface antigens for 30 minutes at 4°C. Cells were washed with FACS buffer and PBS and then fixed overnight (ON) in PBS containing 2% paraformaldehyde. The following antibodies were used: CD4-PB (clone RM4-5, eBioscience), CD8-FITC (clone 5H10-1, Biolegend), CD44-PerCPCy5.5 (clone 1M7, eBioscience), CD62L-PECy7 (clone MEL-14, Biolegend, Ly6G-APC (clone 1A8, Biolegend), MHC II-FITC (clone AMS-32.1,BD Pharmingen), Ly6C-PerCPCy5.5 (clone AL-21,BD Pharmingen), CD11b-PE (clone M1/70 from Biolegend), CD11c-PB (clone N418, Biolegend). Samples were acquired on a LSRII flow cytometer with Diva Software. All data were analyzed using FlowJo version 7.6.5 software. A schematic of the gating strategy performed is depicted below in Figure 4.

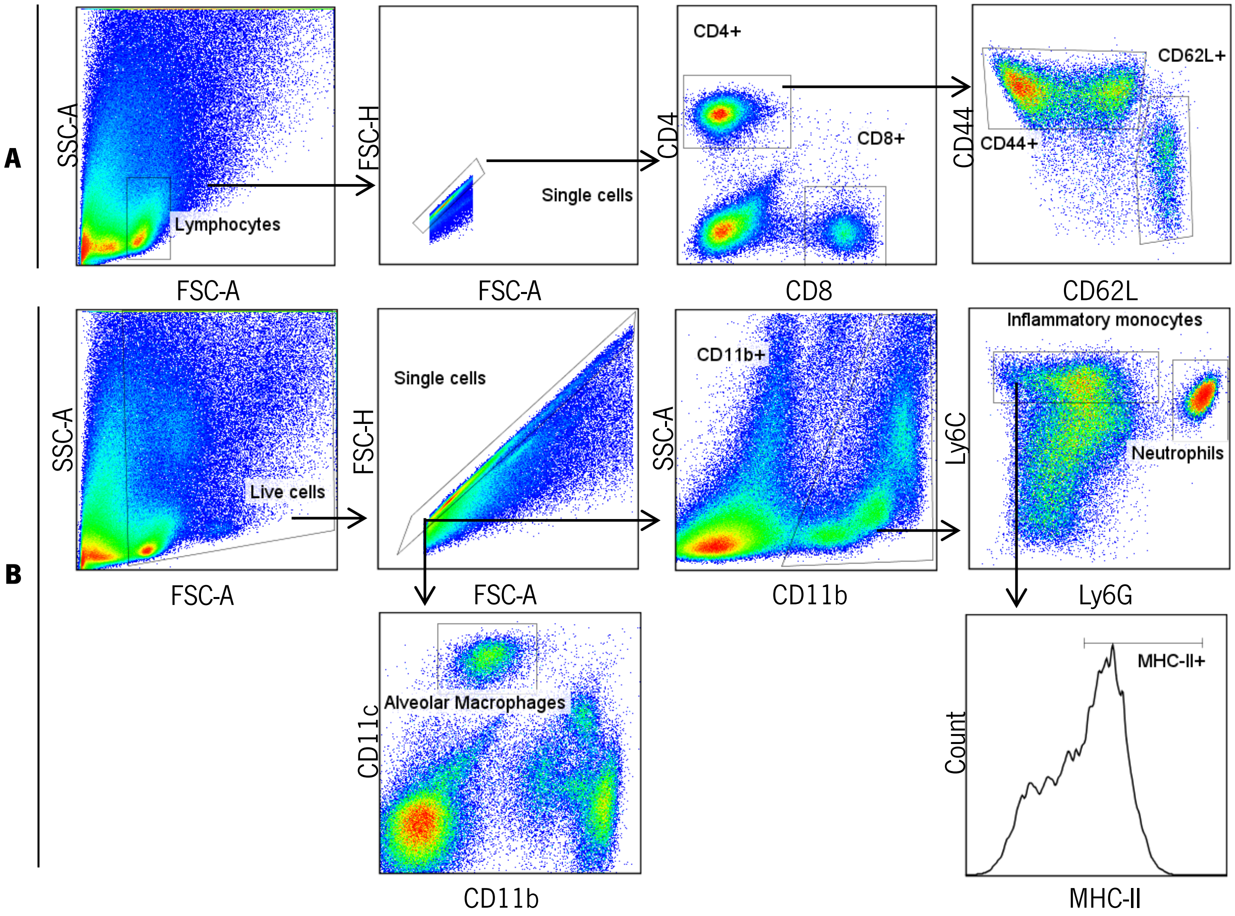

Figure 4: Cytometry analysis. Gating strategy for A) lymphoid cells and B) myeloid cells.

The total number of cells in each gate was calculated using the total number of cells determined by Countess® Automated Cell Counter.

9. Mtb growth curves

H37Rv WT, nrp-complemented and Δnrp mutants were inoculated in 40mL of either 7H9 with 10% OADC or PB medium at an initial OD of 0.002 at 570nm. The cultures were grown in ventilated Erlenmeyers (Cole-Parmer) at 37°C and 120 rpm. Every 48 hours a sample of each culture was used for OD 570nm readings.

10. Cytokine concentration by Enzyme-Linked Immunosorbent Assay (ELISA)

The concentration of TNF-α, IL-1β and IL-10 in the supernatants was determined by using the commercially available ELISA kit for IL-10 (88-7104), IL-1β (88-7013) and TNF-α (88-7324), all from eBioscience, according to the manufacturer's instructions.

11. RNA extraction and quantification

Total RNA from cell suspensions was extracted by using TRIzol® Reagent (Invitrogen, San Diego, CA) according to the manufacturer's instructions. Briefly, glycogen (20μg/μl from Roche) was added to each sample and incubated for 5 minutes at RT. After incubation, 50μl of chloroform (Sigma-Aldrich) were added and the samples were mixed by vortexing and incubated on ice for 15 minutes. Afterwards, samples were centrifuged at 13000 rpm for 15 minutes at 4°C, and the upper aqueous phase was carefully recovered, and mixed with an equal volume of isopropyl alcohol (Sigma-Aldrich) to precipitate the RNA. Samples were incubated ON at -20°C and centrifuged at 13000 rpm for 15 minutes at 4°C. The supernatant was removed and the pellet washed with 800μl of 70% ethanol (Carlo Erba reagents). Ethanol was completely removed after centrifugation at 9000 rpm for 5 minutes and the dried RNA pellet was resuspended in RNase/DNase-free water (Gibco). RNA concentration was measured at 260nm (Nanodrop ND-1000 Spectrophotometer) and the purity assessed through the A260/A280 and A260/A230 ratios.

12. Reverse transcriptase polymerase chain reaction (RT-PCR)

Complementary DNA (cDNA) was synthesized using the GRS cDNA Synthesis Mastermix Kit (GRISP) according to the manufacturer's instructions. Briefly, reaction mix was composed by 10μl of GRS RT Mastermix, 1μl of oligo(dT)$_{20}$ and 9μl of RNA sample mixed with nuclease-free water. The cDNA synthesis reaction was performed in thermocycler (MyCycler, Bio-Rad) with the following program: 25°C for 10 minutes followed by 10 minutes at 42°C and 5 minutes for 85°C. The resultant cDNA template was used for quantification of target genes expression by real-time PCR (RT-PCR) analysis using SYBR green or TaqMan detection systems.

13. Quantitative Real-Time PCR (qRT-PCR)

For SYBR Green reactions 1μL of each cDNA sample was mixed with 9μL of reaction mix containing 3μL of water, 1μL of 0.4μM forward and reverse specific primer and 5μL of SYBR green qPCR Master Mix (GRISP). RT-PCR was performed in CF*96TM Real-time system (Bio-Rad) using the following program: 95°C for 15 minutes, followed by 40 amplification cycles of 95°C for 3 seconds, 60°C for 20 seconds and

70°C for 15 seconds, for melting curve analysis. For TaqMan reactions 1µL of each cDNA sample was mixed with 9µL of reaction mix containg 3.5µL of water, 0.5µL of specific primer-probes and 5µL of TaqMan Gene Expression Master Mix (Applied Biosystems). The RT-PCR program used was 50°C for 2 minutes, 95°C for 10 minutes, 40 cycles of 95°C for 15 seconds and 60°C for 1 minute. Relative mRNA expression of the target gene was normalized to the levels of the housekeeping gene using the ΔCt method: 1.8^(Housekeeping gene mRNA expression – Target gene mRNA expression) x 100000. The sequences of primers and references of the TaqMan primer-probe sets used in RT-PCR are listed in Table 1.

Table 1: Sequences of SYBR Green primers and TaqMan primer-probes used.

SYBR Green primers	Forward	Reverse
Ubiquitin	5'-TGGCTATTAATTATTCGGTCTGCAT-3'	5'-GCAAGTGGCTAGAGTGCAGAGTAA-3'
TNF-α	5'- GCCACCACGCTCTTCTGTCT-3'	5'- TGAGGGTCTGGGCCATAGAAC -3'
IFN-γ	5'-CAACAGCAAGGCGAAAAAGG-3'	5'-GGACCACTCGGATGAGCTCA-3'
IL-1β	5'-TGTAATGAAAGACGGCACACC-3'	5'-TCTTCTTTGGGTATTGCTTGG-3'

	TaqMan Primer-Probes
HPRT	Mm.299281
CCL2	Mm.441242
CCL7	Mm.443113

14. Statistical Analysis

Data were analyzed using GraphPad Prism 6. Depending on the nature of the dataset, differences between groups were analyzed using Student's t-Test or Two-way ANOVA using Sidak's test for multiple comparisons. Survival curves were compared using the Log-rank (Mantel-Cox) test. Differences were considered significant for $p \leq 0.05$ and represented as follows: *$p \leq 0.05$;**$p \leq 0.01$;***$p \leq 0.001$ and ****$p \leq 0.0001$.

RESULTS

1. Initial considerations

The Δnrp mutant and the nrp-complemented strain were generated on a H37Rv background by our collaborator Dr. Apoorva Bhatt (School of Biosciences, University of Birmingham). Our collaborator is currently characterizing the biochemical and functional properties of nrp. From a microbiological standpoint, we have only assessed whether nrp was required for optimal Mtb growth under normal culture conditions. We found no significant differences in growth kinetics between Mtb strains in either PB or 7H9 liquid medium (Figure 5).

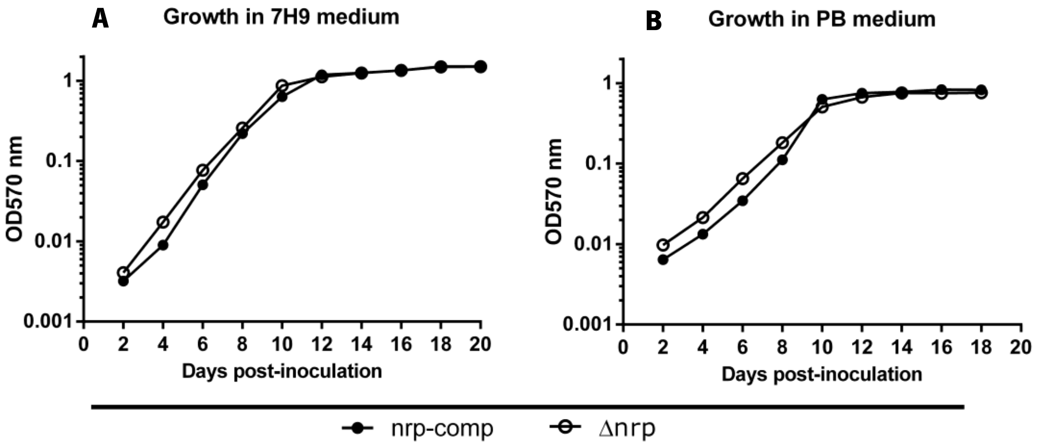

Figure 5: nrp-complemented and Δnrp-mutant strains growth kinetics in liquid media. Biomass over time measured by optic density at 570nm in A) 7H9 and B) PB inoculated with either nrp-complemented or Δnrp-mutant strains. Culture media were inoculated with either Mtb strain at a theoretical OD570nm value of 0.002. Average doubling time in hours (nrp-complemented vs Δnrp-mutant) was 25.15 vs 24.79 in 7H9 medium and 34.92 vs 34.08 in PB medium.

Thus, we focused on characterizing the relevance of this protein in the context of infection. To achieve this goal we took advantage of the mouse model infected via the aerosol route previously established in our laboratory. From these animals we assessed survival and bacterial burdens, gene expression as well as immunopathology in specific organs throughout the course of infection. We have also resorted to infecting macrophages from different origins to further elucidate innate interactions between host cells and pathogen. Overall this experimental setup has allowed us to better understand the role of nrp in the context of infection.

2. *In vivo* infection

2.1. Nrp is required for optimal establishment of infection

To assess the relevance of nrp during infection, we started by infecting via the aerosol route WT C57BL/6 mice with either Δnrp-mutant or nrp-complemented strains. Bacterial burdens in the lung and spleen were analyzed at different time-points throughout infection (Figure 6A and 6B). Our data showed a difference regarding lung bacterial burden by day 20 post-infection between Mtb strains expressing or not *Nrp* (Figure 6A). Specifically, animals infected with the Δnrp-mutant strain presented on average a 48-fold lower bacterial burden (1.683 Log_{10} average difference) when compared to those infected with the nrp-complemented strain.

We have also observed differences regarding bacterial burdens in the spleen of infected animals (Figure 6B). In this organ we were unable to detect Mtb before day 30 post-infection in animals infected with the Δnrp-mutant. Moreover, the bacterial burden shown at day 30 post-infection in these animals remained stable (≈ 3.25 Log_{10}) throughout the time period assessed, significantly lower than the one observed in animals infected with the nrp-complemented strain.

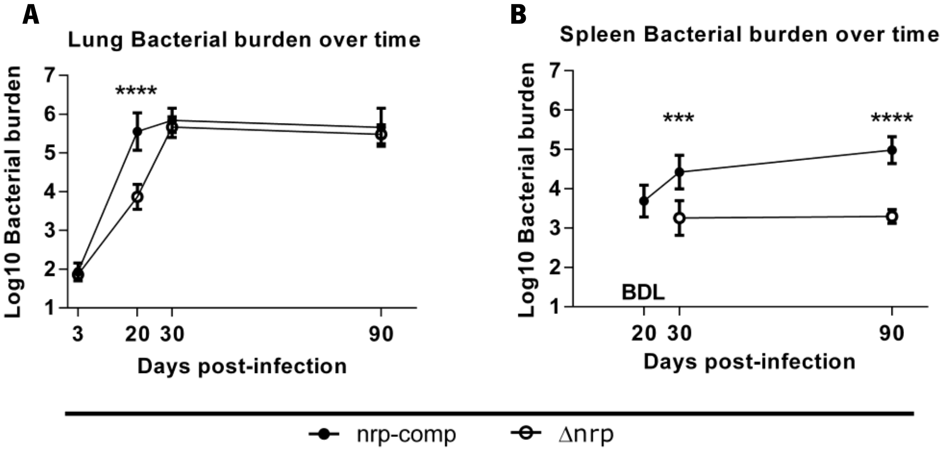

Figure 6: Animals infected with the Δnrp-mutant or the nrp-complemented strain presented different bacterial burdens over time in the lungs and spleen. A) Lung bacterial burden differs between Mtb strains at day 20 between Δnrp and complemented strain (average 3.867 vs 5.550 Log_{10} bacterial burden, respectively). **B)** Spleen bacterial burden in Δnrp-mutant infected mice was lower for every time-point assessed when compared to mice infected with the nrp-complemented strain. Data analyzed performing a Two-way ANOVA using Sidak's test for multiple comparisons. BDL – Below detection level.**** p<0.0001 *** p<0.001; **p<0.01. Each time-point contains pooled data from 2 separate experiments with 5 animals each. Initial bacterial burden for animals infected with the Δnrp-mutant and the nrp-complemented strain were 1.860±0.0446 Log_{10} and 1.931±0.0822 Log_{10}, respectively.

Taken together, these data suggest that nrp is required for Mtb to efficiently colonize the host lungs during early stages of infection in addition to potentiate early dissemination events or facilitating the growth of Mtb in different microenvironments, such as those found in the spleen.

2.2. Nrp induces lung immunopathology

In addition to the differences observed regarding bacterial burdens, a discernible phenotype was also observed in lung histopathological features throughout infection (Figure 7A). In this matter, H&E histological preparations from the lungs of animals infected with either the Δnrp-mutant of the nrp-complemented strain at different time-points throughout infection revealed differences regarding the onset of pathology and the extension of lesions. Specifically, by day 20 post-infection no discernible lesions were observed in the lungs of Δnrp-mutant infected animals, whereas multiple small inflammatory infiltrates were already present in the lungs of animals infected with the nrp-complemented strain (Figure 7). This difference was likely due to the differences in bacterial burdens at this time-point (Figure 6A). By day 30 post-infection, lesions in the lungs of mice infected with the nrp-complemented strain were larger than its Δnrp-mutant counterpart, even though both presented the same bacterial burden (Fig 6A). Remarkably, these differences were kept during the chronic stage of infection. Indeed, on day 90 post-infection animals infected with the nrp-complemented strain still presented a greater degree of pathology than those infected with the Δnrp-mutant (Figure 7), despite the fact that bacterial burdens had been similar in both cases for 60 days (Figure 6A).

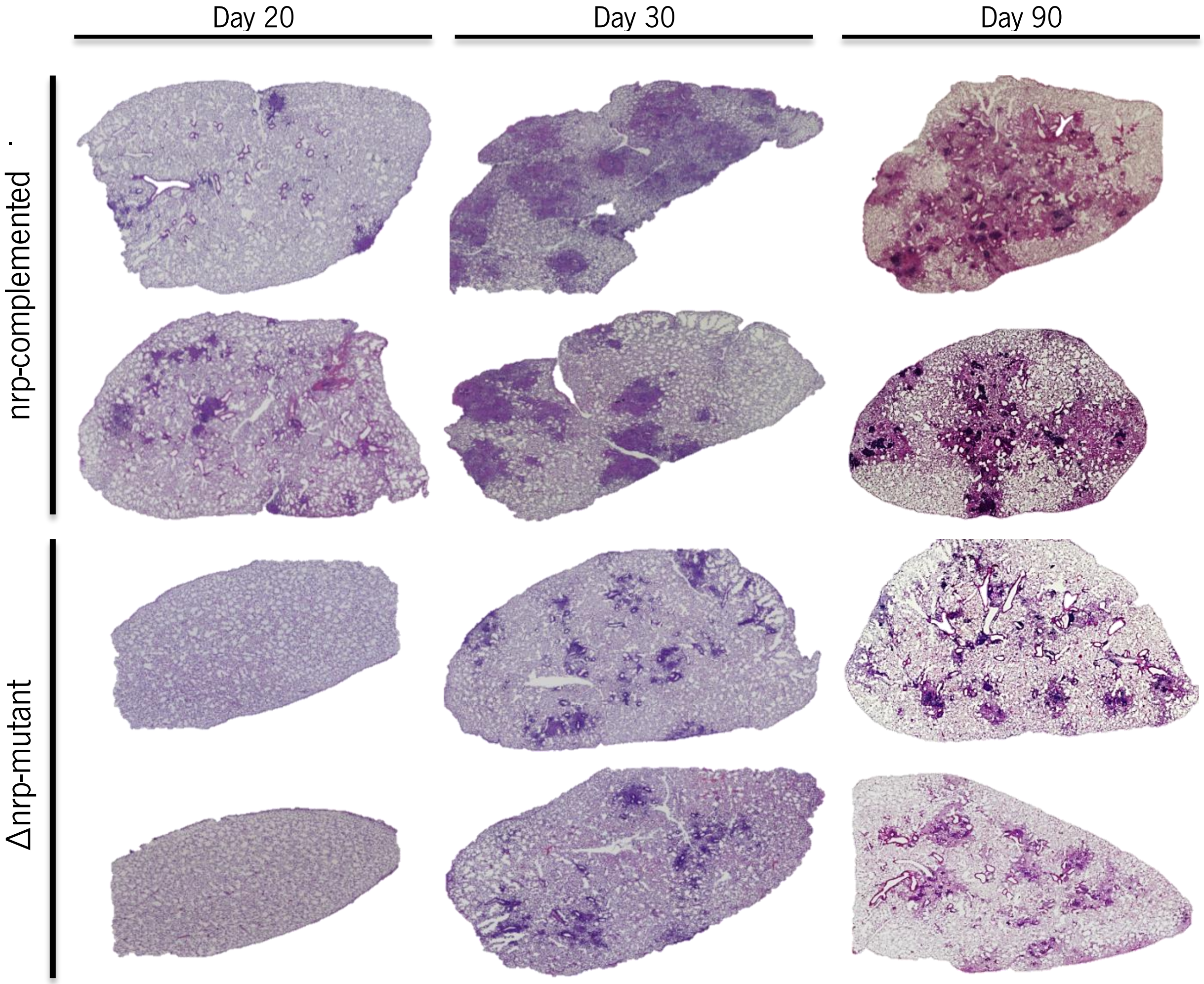

Figure 7: Animals infected with the Δnrp-mutant or the nrp-complemented strain presented different immunopathology in the lungs. H&E stained lung preparations magnified 40X. Initial bacterial burden for animals infected with the Δnrp-mutant and the nrp-complemented strain were 1.860±0.0446 Log_{10} and 1.931±0.0822 Log_{10}, respectively.

Quantification of the percentage of the lung section presenting an inflammatory infiltrate substantiated these observations (Figure 8A), as this area was always higher in mice infected with the nrp-complemented strain than in those infected with the Δnrp-mutant. Furthermore, translating these areas into a previously described histopathological score for lung infection in the mouse model[122] upheld the same differences (Figure 8B).

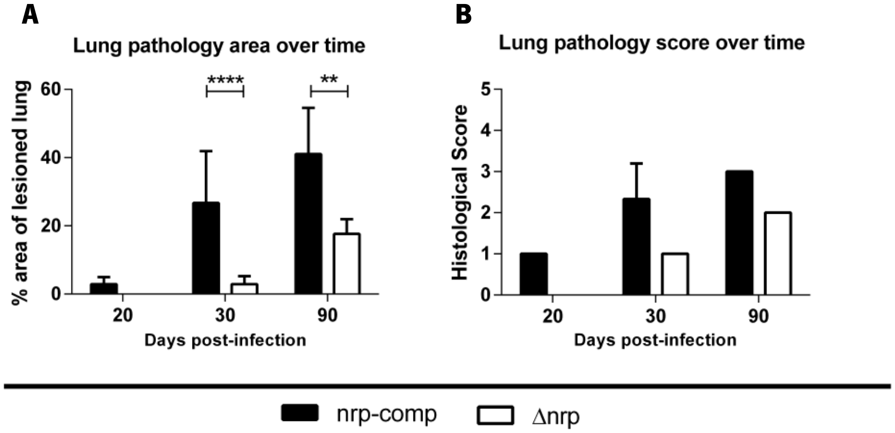

Figure 8: Characterization of H&E preparations from the lungs of animals infected with the Δnrp-mutant or the nrp-complemented strain revealed differences in immunopathology. A) Percentage of lesioned lung area in mice infected with either Δnrp-mutant or nrp-comp Mtb strains. **B)** Lung histopathological score based on the percentage of lesioned lung area. Data analyzed performing a Two-way ANOVA using Sidak's test for multiple comparisons. BDL – Below detection level. **** $p<0.0001$; **$p<0.01$. Each time-point contains pooled data from 2 separate experiments with 5 animals each. Initial bacterial burden for animals infected with the Δnrp-mutant and the nrp-complemented strain were 1.860±0.0446 Log_{10} and 1.931±0.0822 Log_{10}, respectively.

Taken together our data indicate that in the absence of nrp, mice are at least equally able to control infection, doing so with less immunopathology. This suggests that a differential immune response is occurring in the absence of nrp. In turn, this response could account for the lower bacterial burden at day 20 post-infection and the overall lower lung immunopathology observed in mice infected with the Δnrp-mutant, when compared to those infected with the nrp-complemented strain. To assess this hypothesis we proceeded to quantify and characterize by flow cytometry some of the key cell types involved in the immune response to Mtb.

2.3. Immune response characterization

2.3.1. Nrp modulates the cellular immune response

To investigate the hypothesis that distinct immune responses are elicited in the host depending on Mtb expressing *Nrp* or not, we started by analyzing by flow cytometry the dynamics of the different immune cell types in the lungs of infected animals. For this analysis we focused on cells from myeloid and lymphoid origin known to be relevant to the pathogenesis of TB. Accordingly, we assessed different types of phagocytes and CD4+ T cells, as well as some of their activation markers.

By day 20 post-infection, animals infected with the nrp-complemented strain presented an average 5.93-fold higher number of inflammatory monocytes, as defined by the surface markers CD11b+Ly6ChiLy6G-, than their Δnrp-mutant infected counterparts (Figure 6B). Furthermore, these cells presented a higher activation status on nrp-complemented infected animals, as seen by the expression of MHC-II on their surface (Figure 9C). On average, 34.79% of these cells present surface MHC-II class molecules, whereas only an average of 3.41% of inflammatory monocytes from mice infected with the Δnrp-mutant display this marker (data not shown). At day 30 post-infection these differences were attenuated, but were still significant (Figure 9B and 9C). We have observed no significant differences regarding neutrophils, as defined by the surface markers CD11b+Ly6CintLy6Ghi, in any time-point assessed (Figure 9D).

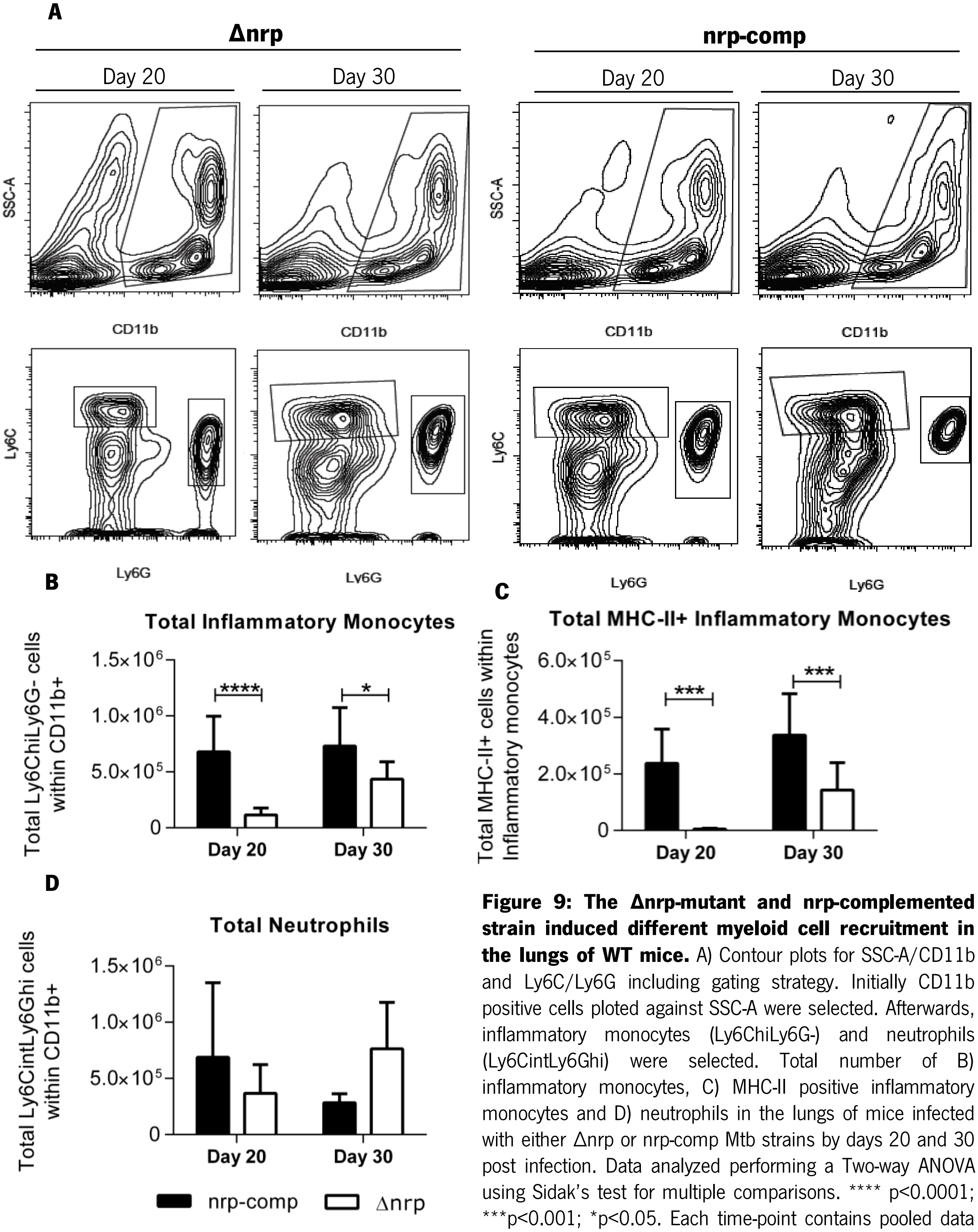

Figure 9: The Δnrp-mutant and nrp-complemented strain induced different myeloid cell recruitment in the lungs of WT mice. A) Contour plots for SSC-A/CD11b and Ly6C/Ly6G including gating strategy. Initially CD11b positive cells ploted against SSC-A were selected. Afterwards, inflammatory monocytes (Ly6ChiLy6G-) and neutrophils (Ly6CintLy6Ghi) were selected. Total number of B) inflammatory monocytes, C) MHC-II positive inflammatory monocytes and D) neutrophils in the lungs of mice infected with either Δnrp or nrp-comp Mtb strains by days 20 and 30 post infection. Data analyzed performing a Two-way ANOVA using Sidak's test for multiple comparisons. **** $p<0.0001$; ***$p<0.001$; *$p<0.05$. Each time-point contains pooled data from 2 separate experiments with 5 animals each. Initial bacterial burden for animals infected with the Δnrp-mutant and the nrp-complemented strain were 1.860±0.0446 Log_{10} and 1.931±0.0822 Log_{10}, respectively.

In contrast with inflammatory monocytes and neutrophils that are recruited to the infected tissue, no differences were observed regarding the resident population of alveolar macrophages, as defined by the surface markers CD11chiCD11blow (Figure 10B).

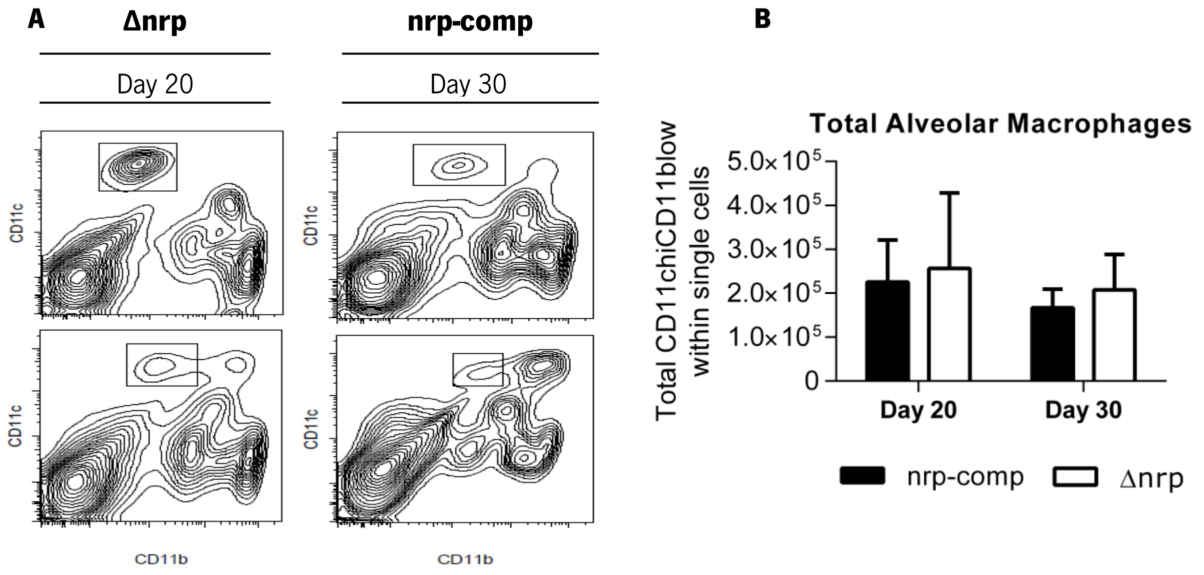

Figure 10: Total number of alveolar macrophages was independent of infecting strain. A) Contour plots for CD11c/CD11b including gating strategy. Gating was performed on CD11chiCD11bint. **B)** Total number of alveolar macrophages in the lungs of mice infected with either Δnrp or nrp-comp Mtb strains by days 20 and 30 post-infection. Data analyzed performing a Two-way ANOVA using Sidak's test for multiple comparisons. Each time-point contains pooled data from 2 separate experiments with 5 animals each. Initial bacterial burden for animals infected with the Δnrp-mutant and the nrp-complemented strain were 1.860±0.0446 Log$_{10}$ and 1.931±0.0822 Log$_{10}$, respectively.

Analysis of CD4+ lymphocytes revealed differences regarding both total number and activation status. Specifically, and although non-significant, by day 20 post-infection the lungs of animals infected with the nrp-complemented strain presented higher numbers of CD4+ T cells (≈ 2-fold) than those infected with the Δnrp-mutant (Figure 11B). This trend was also translated in total number of activated CD4+ lymphocytes (Figure 11C), defined by the surface markers CD4+CD44+CD62L-, as animals infected with the nrp-complemented strain presented higher numbers of this cell type than those infected with the Δnrp-mutant (average 4-fold difference). By day 30 post-infection we observed significant differences between these cell types depending on the infecting Mtb strain (Figure 11). In this regard, animals infected with the nrp-complemented strain presented approximately 2.25 times more CD4+ T cells and 2.84 times more activated CD4+ T cells than animals infected with the Δnrp-mutant.

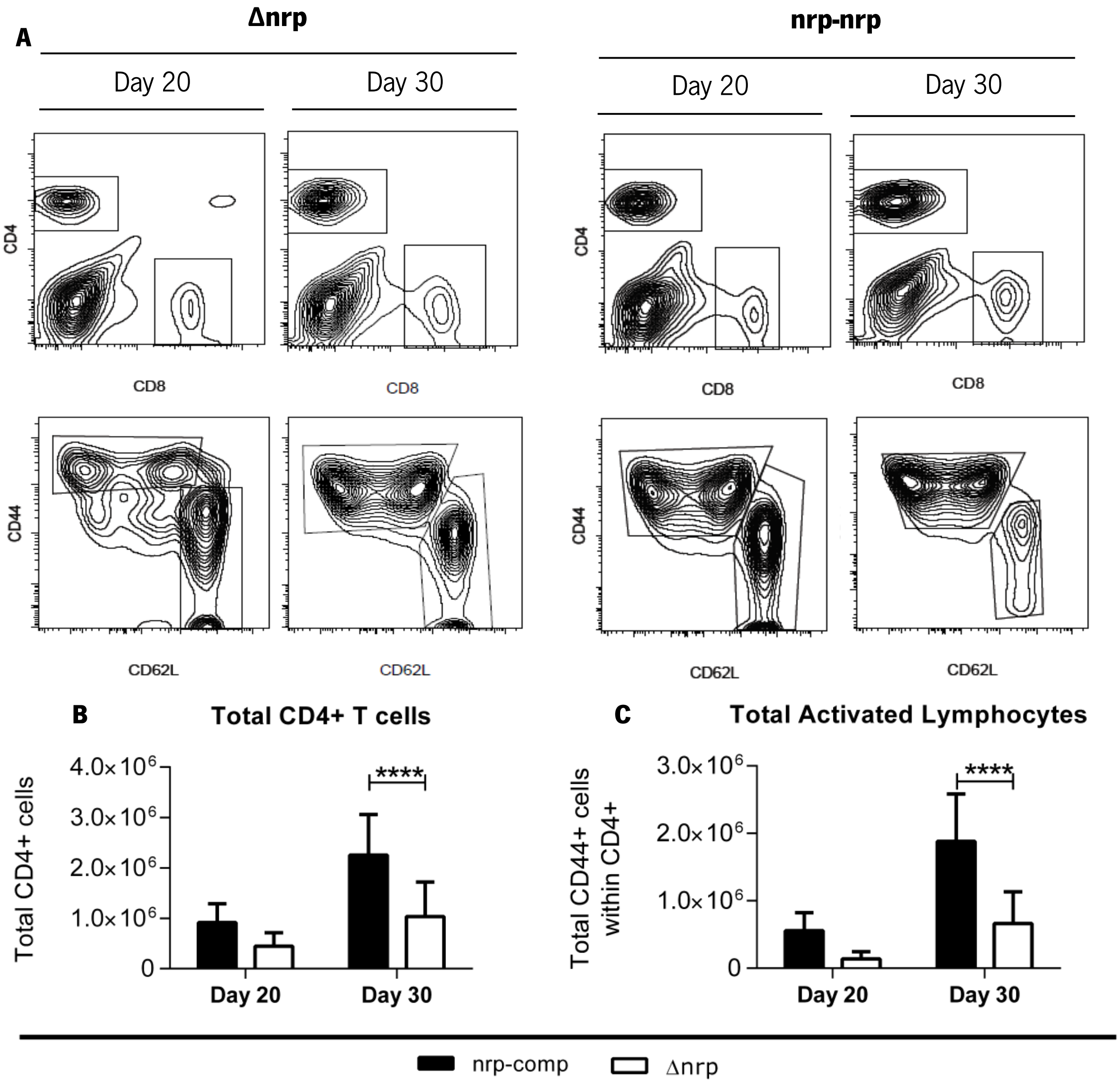

Figure 11: The Δnrp-mutant and nrp-complemented strains present different CD4+ T cell features in the lungs of WT mice. A) Contour plots for CD4/CD8 and CD44/CD62L including gating strategy. Initially CD4 positive cells ploted against CD8 were selected. Afterwards, activated lymphocytes (CD44hiCD62L-) and non-activated lymphocytes (CD44-CD62Lhi) were selected. **B)** Total number of CD4+ T cells and **C)** activated CD4+ lymphocytes in the lungs of mice infected with either Δnrp or nrp-comp Mtb strains by days 20 and 30 post-infection. Data analyzed performing a Two-way ANOVA using Sidak's test for multiple comparisons. **** $p<0.0001$. Each time-point contains pooled data from 2 separate experiments with 5 animals each. Initial bacterial burden for animals infected with the Δnrp-mutant and the nrp-complemented strain were 1.860±0.0446 Log_{10} and 1.931±0.0822 Log_{10}, respectively.

Taken together, the cytometry data suggest that expression of nrp by Mtb induces a stronger immune response, since in its presence most cell types involved in the immune response against Mtb are present in higher numbers and with a higher activation status throughout infection. Nevertheless, this vigorous immune response does not appear to be beneficial for the host, since it is not translated into a better control of Mtb and is actually accompanied by enhanced immunopathology. Indeed, in the absence of nrp, a milder immune response seems to be better able to control Mtb up to day 30 post-infection. This phenotype raises the question of how nrp orchestrates the mounting of an immune response to the advantage of Mtb and how this response differs in terms of key molecular agents in the absence of nrp. To address this issue we assessed the expression of several molecules relevant in the immune response against Mtb.

2.3.2. Cytokine and chemokine expression is modulated by nrp

To clarify the differences observed regarding cell numbers, we chose to analyze the chemokines CCL2 and CCL7, as these are known to play a role in recruitment of immune cells to the site of infection and in assisting the triggering of an adaptive immune response[60]. Moreover, to elucidate whether nrp induces functional differences in the immune response, other than cell numbers, we assessed the expression of TNF-α, IL-1β, IFN-γ, NOS2 and IL-17 at the site of infection. Among these, TNF-α, IL-1β and IFN-γ are essential to fully activate the host microbicidal mechanisms and NOS2 is responsible for the production RNS, one of the main defense mechanisms against Mtb. Additionally, we also examined IL-17 expression, as differences in this cytokine may reflect a differential polarization of T cells between the Th1 and Th17 phenotype.

Interestingly, *Ccl2* expression was lower in animals infected with the Δnrp-mutant by day 20 post-infection than in animals infected with the nrp-complemented strain (Figure 12A). This chemokine is responsible for the recruitment of myeloid cells to the site of infection, especially monocytes and DCs. Furthermore, it also plays a role on the migration of APCs to the lymph node, therefore contributing to the generation of an adaptive immune response[5]. The fact that the expression of this chemokine was reduced in animals infected with the Δnrp-mutant by day 20 post-infection is in line with the lower number of inflammatory monocytes and CD4+ lymphocytes present, when compared to animals infected with the nrp-complemented strain (Figure 9B and 11). On the other hand, the relative expression levels of this chemokine shifts by day 30 post-infection. In this case, Δnrp-mutant infected mice expressed higher levels of CCL2 when compared with their nrp-complemented infected counterparts. This increase in *Ccl2* coincides with an increased recruitment of inflammatory monocytes to the lungs of Δnrp-mutant infected mice. Although not significant, a similar profile of expression was observed for *Ccl7* (Figure 12B), a close relative of *Ccl2*, which may therefore contribute to the lower levels of inflammatory monocytes observed in the lungs of mice infected with the Δnrp-mutant.

Interestingly, and despite the 48-fold lower bacterial burden observed in animals infected with the Δnrp-mutant by day 20 post-infection, when compared to nrp-complemented infected mice, there appears to be no difference on the expression levels of *Tnf* and *Il1b* (Figure 12C and 12D). A possible scenario is that the Δnrp-mutant activates the innate immune cells to induce higher levels of these cytokines. This would explain why despite the lower bacterial burden by day 20, mice infected with the Δnrp-mutant expressed similar levels of these cytokines when compared to mice infected with the nrp-complemented strain. By day 30, mice infected with the Δnrp-mutant express lower levels of *Il1b* and higher levels of *Tnf* when compared to mice infected with the nrp-complemented strain.

Finally, the lung expression of *Ifng* (Figure 12E) on day 20 post-infection was lower for the Δnrp-mutant than for the nrp-complemented strain. These differences subsided by day 30 post-infection. At this time-point, IFN-γ expression reached similar levels to those observed in animals infected with the nrp-complemented strain on day 20 post-infection. As previously mentioned, the expression of *Nos2* and *Il17* were also assessed, but no measureable amplification was observed in either time-point assayed.

Taken together, these gene expression assays revealed that expression of nrp during infection induced the recruitment of innate immune cells likely in a CCL2, and to a lesser extent CCL7, dependent-way. Furthermore, nrp expression also led to a differential activation of immune cells, as seen by the distinct expression of *Tnf* and *Il1β* between animals infected with Mtb expressing nrp or not. Lastly, nrp also appeared to anticipate the onset of a Th1 response, as seen by the earlier expression of IFN-γ in animals infected with the nrp-complemented strain.

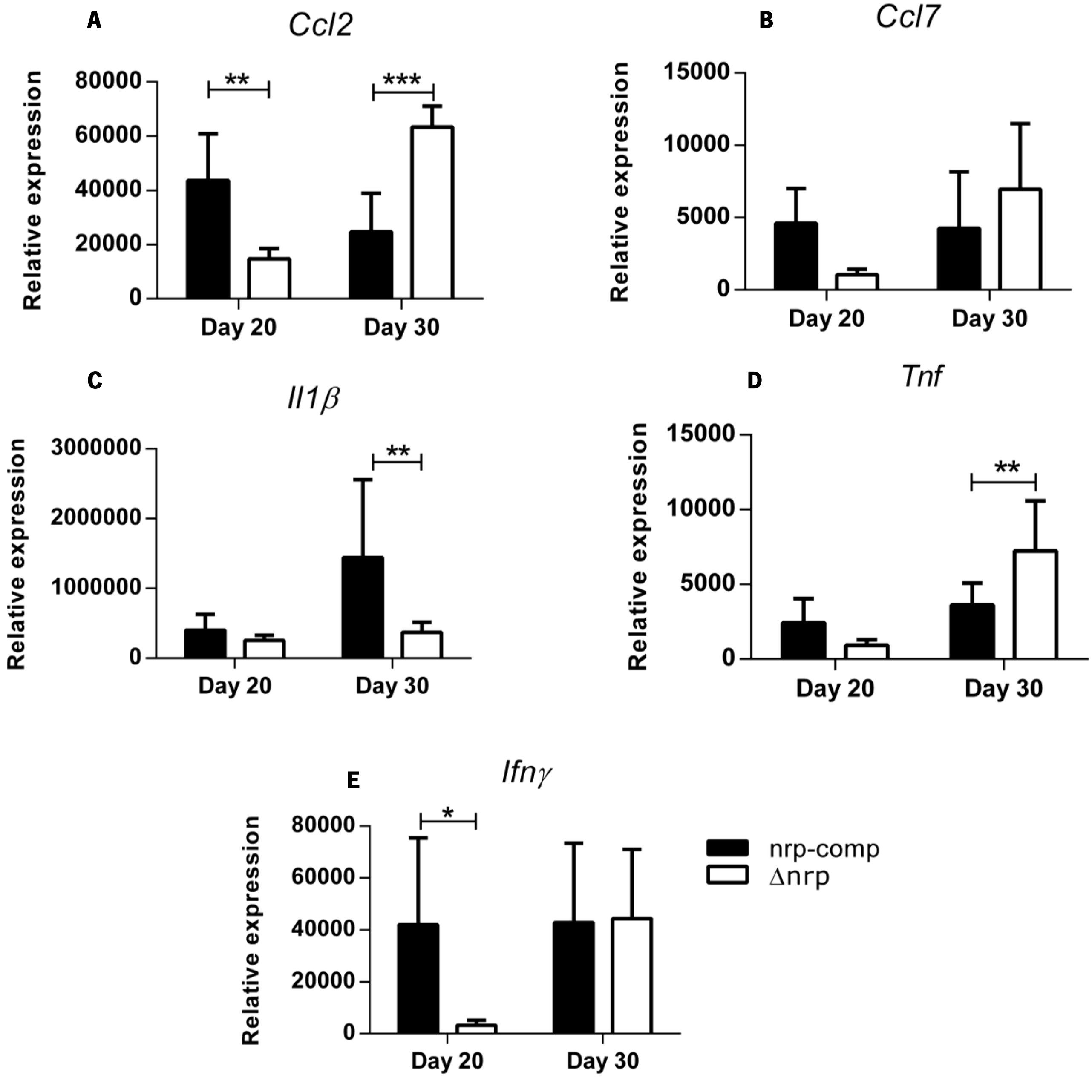

Figure 12: The Δnrp-mutant and nrp-complemented strain induced differential cytokine/chemokine expression in the lungs of WT mice. Expression of **A)** *Ccl2* **B)** *Ccl7* **C)** *Il1β* **D)** *Tnf* and **E)** *Ifnγ* relative to *Hprt* in the lungs of mice infected with either Δnrp-mutant or nrp-complemented Mtb strains by days 20 and 30 post-infection. Data analyzed performing a Two-way ANOVA using Sidak's test for multiple comparisons. *** $p<0.001$; **$p<0.01$;*$p<0.05$. Each time-point contains pooled data from 2 separate experiments with 5 animals each. Initial bacterial burden for animals infected with the Δnrp-mutant and the nrp-complemented strain were 1.860±0.0446 Log_{10} and 1.931±0.0822 Log_{10}, respectively.

2.3.3. Nrp is required for full virulence in mouse models of deficient adaptive immunity

Taking into consideration that, in WT mice, differences in bacterial burden were only detected on day 20 post-infection, a period of time where the immune response is predominantly innate, we next investigated the contribution of the adaptive immune response in the context of infection with Mtb expressing or not nrp. For this purpose, we infected RAG-2 deficient mice, which are unable of generating B and T lymphocytes, and IFN-γ deficient animals, which lack the expression of IFN-γ a key protective mechanism against Mtb.

RAG-2 deficient animals are unable to control Mtb growth and typically succumb to infection 40 to 50 days after infection [73]. Accordingly, RAG-2 deficient mice infected with the nrp-complemented strain showed an average survival of 44.7 days (Figure 13A). Interestingly, RAG-2 deficient mice infected with the Δnrp-mutant presented an average survival of 114 days post-infection (Figure 13A). These data clearly point nrp as a virulence factor. We also followed the bacterial burdens of RAG-2 deficient animals at different stages of infection (Figure 13B). Consistently with the absence of an adaptive immune response the bacterial burden in the lungs of RAG-2 deficient animals infected with Mtb expressing or not nrp kept increasing over time. Specifically, lung bacterial burden in RAG-2 deficient animals infected with the nrp-complemented strain or the Δnrp-mutant increased steadily until reaching an average of 8.01 Log_{10} and 8.29 Log_{10}, respectively, before succumbing to infection (Figure 13B). Additionally, without the control provided by an adaptive immune response, RAG-2 deficient animals infected with the nrp-complemented strain presented a higher bacterial burden from day 20 onward than those infected with the Δnrp-mutant.

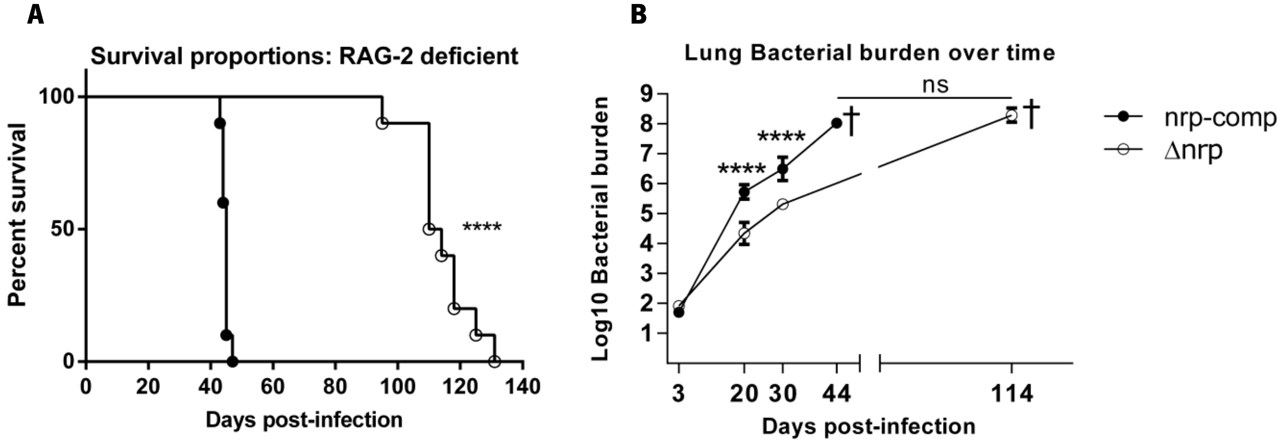

Figure 13: The Δnrp-mutant presented reduced virulence in RAG-2 deficient mice. A) Survival curve of RAG-2 deficient mice infected with either the nrp-complemented strain or Δnrp-mutant, using 10 animals per strain. **B)** Bacterial burden over time of RAG-2 deficient infected with either Mtb strain. Terminal bacterial burden ploted on the average survival time and marked with a black cross. Each time-point contains data from 5 animals. ****p<0.0001. ns – non-significant. Initial bacterial burden for animals infected with the Δnrp-mutant and the nrp-complemented strain were 1.920±0.069 Log$_{10}$ and 1.701±0.0707 Log$_{10}$, respectively.

A similar phenotype was observed by infecting IFN-γ deficient animals (Figure 14). In this case, animals infected with the Δnrp-mutant had an average survival of 99 days, whereas those infected with the nrp-complemented strain registered an average survival of 45 days (Figure 14A). Furthermore, animals infected with either strain had the same terminal bacterial burden, 8.357 vs 8.203 Log$_{10}$for Δnrp-mutant and nrp-complemented infected animals, respectively (Figure 14B). Interestingly, animals infected with either strain displayed distinct immunopathological features at the time of death (Figure 14C and 14D). Notably, the differences in the histological phenotype observed in IFN-γ deficient animals infected with either strain resemble those observed in WT mice, where animals infected with the Δnrp-mutant mutant develop smaller lesions than those infected with the nrp-complemented strain.

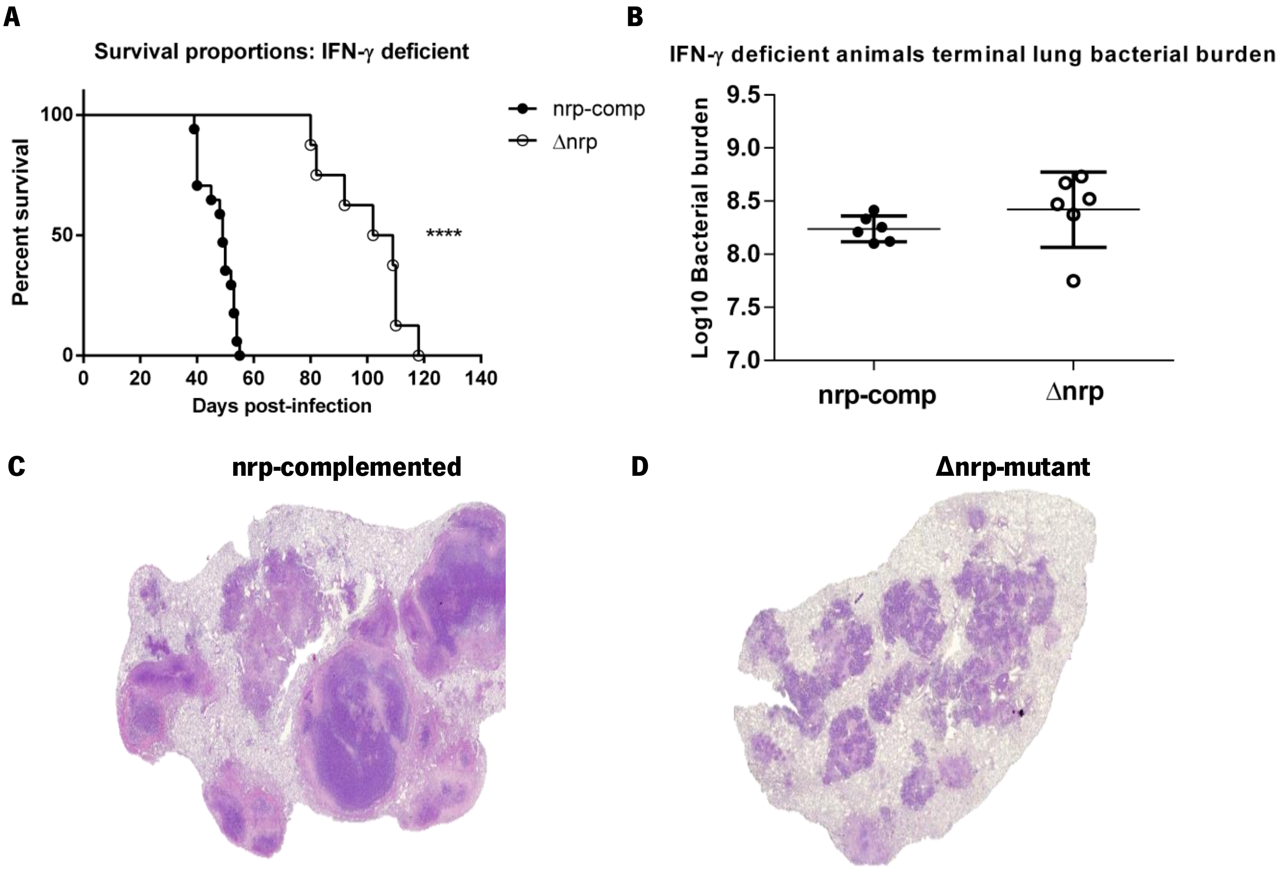

Figure 14: The Δnrp-mutant presented reduced virulence in IFN-γ deficient mice. A) Survival curve of IFN-γ deficient mice infected with either the Δnrp-mutant or the nrp-complemented strain, using 8 animals per curve. **B)** Bacterial burden of IFN-γ deficient animals at the time of death. H&E preparations of terminally ill IFN-γ deficient mice infected with **C)** the nrp-complemented strain and **D)** Δnrp-mutant magnified 40X. The presented images are representative of the entire group. Kaplan-Meier curves analyzed using the log-rank (Mantel-Cox) test. ****p<0.0001. Initial bacterial burden for animals infected with the Δnrp-mutant and the nrp-complemented strain were 1.920±0.069 Log_{10} and 1.748±0.0707 Log_{10}, respectively.

Taken together, the data regarding the survival of animals with severely compromised or absent adaptive immunity show that nrp expression increased the virulence of Mtb, possibly by allowing the bacterium's proliferation inside innate immune cells. Whether this is due to a circumvention of innate microbicidal mechanisms or an increased resistance to those mechanisms is the main question that arises from this part of the work and that we are currently investigating.

2.3.4. Innate immune deficiencies

So far, we have showed that in the absence of nrp the innate immunity is better able to control Mtb. Specifically, the Δnrp-mutant presents a slower growth in both mouse models of deficient adaptive immunity and during the innate phase of the immune response in WT mice when compared to the nrp-complemented strain. In line with this, we proceeded to explore innate immune pathways that may account for the superior control over Mtb lacking nrp. For this purpose, we infected different mouse strains, available in our laboratory, deficient for the main surface TLRs involved in the recognition of Mtb, and in inflammatory mediators relevant in the early response this pathogen.

2.3.4.1. Nrp-dependent virulence is not mediated by TLR-2 or TLR-4 activation

To assess whether the improved control of the Δnrp-mutant during the innate phase of the immune response (approximately the first 3 weeks post-infection) was dependent on signaling through TLR-2 or TLR-4, the main surface TLRs responsible for recognizing Mtb, we started by infecting mice deficient in either of these receptors. No significant differences regarding lung bacterial burdens were observed between these strains and WT mice (Figure 15A and 15B). Together, these data show that nrp is unlikely to modulate interactions between Mtb and the main surface TLRs responsible for recognizing this pathogen.

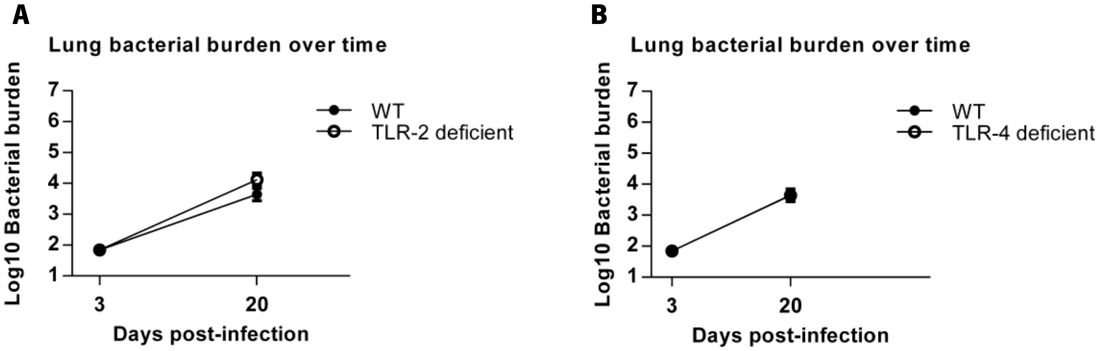

Figure 15: nrp does not appear to modulate the recognition of Mtb by immune cells through TLR-2 and TLR-4. Lung bacterial burden over time in **A)** TLR-2 and **B)** TLR-4 deficient animals infected with the Δnrp-mutant. Data analyzed performing a Two-way ANOVA using Sidak's test for multiple comparisons. Each time-point contains data from 5 animals. Initial bacterial burden for animals infected with the Δnrp-mutant was 1.920±0.069 Log_{10}.

2.3.4.2. Nrp-dependent virulence is not mediated by the eicosanoid pathway

Next we explored the eicosanoid pathway, as it has been reported that shifting arachidonic acid metabolism towards PGE2 production, in detriment of LTB4 and LXA4, results in a better control of infection [47,51]. Accordingly, we infected ALOX 5 deficient mice which lack production of both LTB4 and LXA4, and ALOX 15 deficient mice, which lack LXA4 production, with the Δnrp-mutant. We observed no significant differences regarding lung bacterial burden between these strains and WT mice (Figure 16A and 16B).

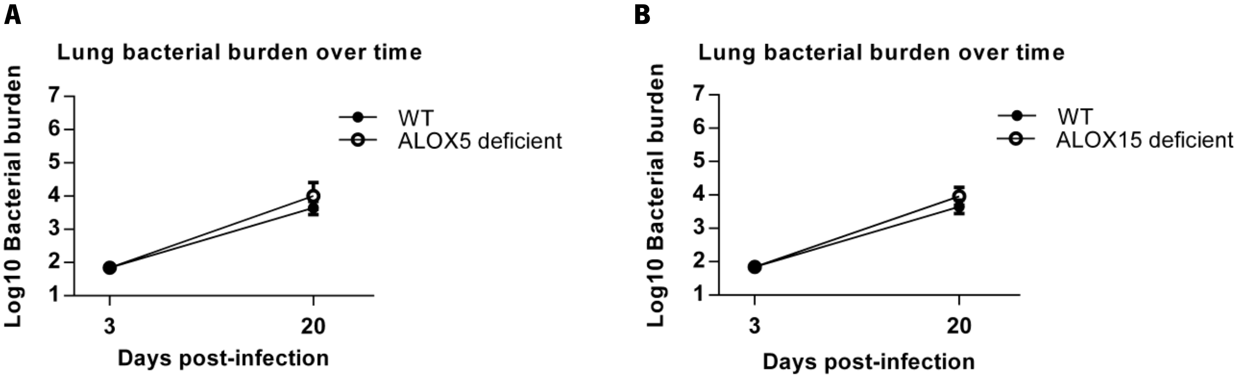

Figure 16: Shifting the eicosanoid pathway towards PGE2 production did not seem to impact control of the Δnrp-mutant. Lung bacterial burden over time in **A)** ALOX 5 and **B)** ALOX 15 deficient animals infected with the Δnrp-mutant. Data analyzed performing a Two-way ANOVA using Sidak's test for multiple comparisons. Each time-point contains data from 5 animals. Each time-point contains data from 5 animals. Initial bacterial burden for animals infected with the Δnrp-mutant was 1.920±0.069 Log_{10}.

One possible scenario would be that the Δnrp-mutant was selectively triggering PGE2 production, hence no phenotype would be observed by removing LTB4 or LXA4. To further investigate this hypothesis, ALOX 5 and ALOX 15 deficient animals were infected with the nrp-complemented strain. This was not the case, as both ALOX 5 and ALOX 15 deficient animals displayed similar lung bacterial burdens as WT mice when infected with the nrp-complemented strain (Figure 17A and 17B).

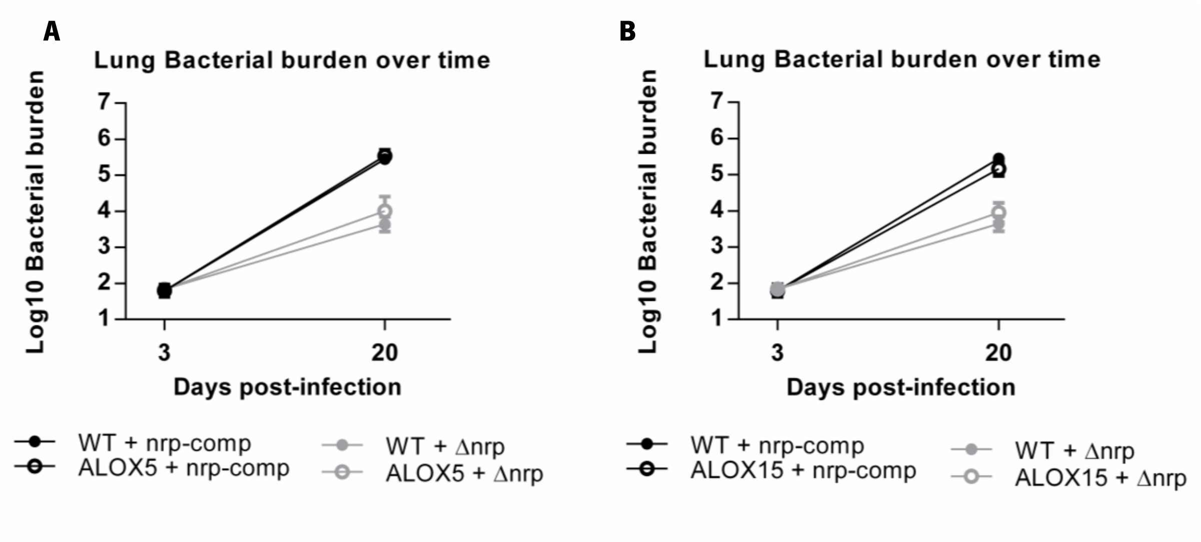

Figure 17: The eicosanoid pathway was not modulated by nrp. Lung bacterial burden over time in **A)** ALOX 5 and **B)** ALOX 15 deficient animals infected with either the Δnrp-mutant or the nrp-complemented strain. Data analyzed performing a Two-way ANOVA using Sidak's test for multiple comparisons. Each time-point contains data from 5 animals. Initial bacterial burden for animals infected with the Δnrp-mutant and the nrp-complemented strain were 1.920±0.069 Log_{10} and 1.701±0.071 Log_{10}, respectively.

In summary, we showed that the phenotype observed in the absence of nrp is not due to a differential activation of innate immune cells via the main surface TLRs involved in Mtb recognition. Additionally, we have shown that the eicosanoid pathway is uninvolved with our phenotype.

3. *in vitro* studies

Considering all our data, it is clear that the phenotype observed with the Δnrp-mutant occurs mainly during the innate phase of the immune response and is independent of TLR recognition and the eicosanoid pathway. To gain further insights on the mechanistic bases of this phenotype we next explored the *in vitro* infection of macrophages. We started by infecting BMDMs at a MOI of 1 in the presence or absence of IFN-γ. BMDMs without IFN-γ activation should resemble macrophages during the innate phase of the immune response, whereas macrophages activated with this cytokine should resemble those found after the onset of the adaptive immune response. We found that BMDMs activated with IFN-γ appear to be equally capable controlling the Δnrp-mutant and the nrp-complemented Mtb strains (Figure 18A, 18B and 18C). However, in the absence of IFN-γ the bacterial growth differed depending on the expression of nrp. Specifically, the number of viable nrp-complemented bacteria increased 0.2 Log_{10} between 4 and 96 hours post-infection

(Figure 18A and 18C), whereas no changes in the number of viable Δnrp-mutant bacteria were observed between these time-points (Figure 18B and 18C).

Similar results were obtained by infecting thioglycolate induced peritoneal macrophages (Figure 18D), a terminally differentiated type of macrophages. In this case, although both strains showed growth 96h post-infection, this was on average 0.31 Log_{10} higher for the nrp-complemented strain. Unlike the results observed at 48h post-infection in BMDMs, peritoneal macrophages were better able to initially control the Δnrp-mutant. Specifically, the number of viable bacteria decreased at 48 hours post-infection for Δnrp-mutant and nrp-complemented strains, but this decrease was on average 0.22 Log_{10} for the Δnrp-mutant (Figure 18D).

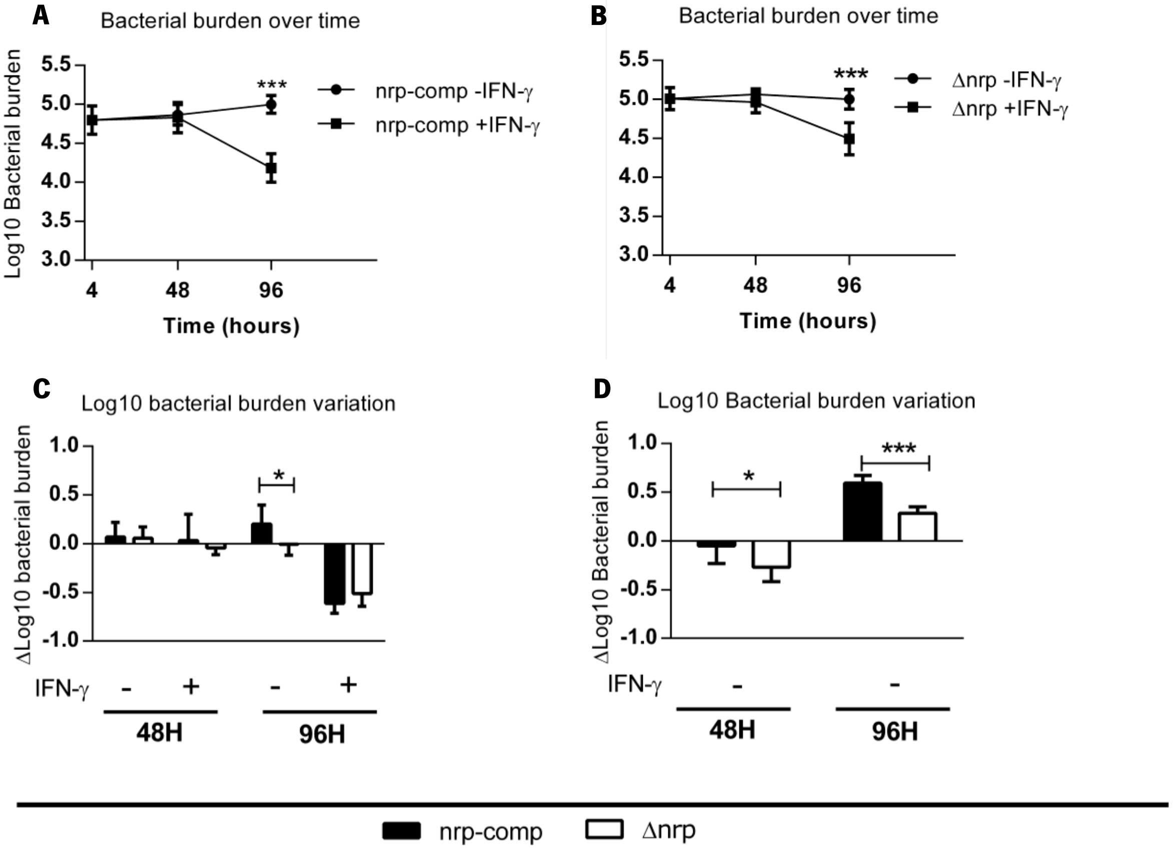

Figure 18: nrp was required for optimal Mtb growth inside macrophages but did not protect against IFN-γ dependent mechanisms. Bacterial burden over time in BMDM infected with the **A)** Δnrp-mutant or the **B)** nrp-complemented strain in the presence or absence of 100U/mL of IFN-γ. Variation of bacterial burden over time relative to 4 hours post-infection in **C)** BMDMs and **D)** thioglycolate induced peritoneal macrophages. Data analyzed performing a Two-way ANOVA using Sidak's test for multiple comparisons. Each time-point contains pooled data from 2 separate experiments. ***p<0.001; *p<0.05

These *in vitro* data suggest that the differences observed *in vivo* may be largely due to the bacterium being less fit to proliferate within the phagocyte. One possibility is that nrp modulates the activation of the macrophage, making it a more permissive environment for the growth of the bacterium.

To assess this hypothesis, we evaluated whether the production of RNS and inflammatory cytokines in BMDMs infected with Mtb expressing or not nrp. Our data showed that that as early as 48 hours after infection, BMDMs infected with the Δnrp-mutant, but not those infected with the nrp-complemented strain, produce measureable levels of nitrites (Figure 19A and 19B). These differences are sustained until 96 hours after infection (Figure 19B). In contrast, upon IFN-γ addition no differences were observed (Figure 19C and 19D).

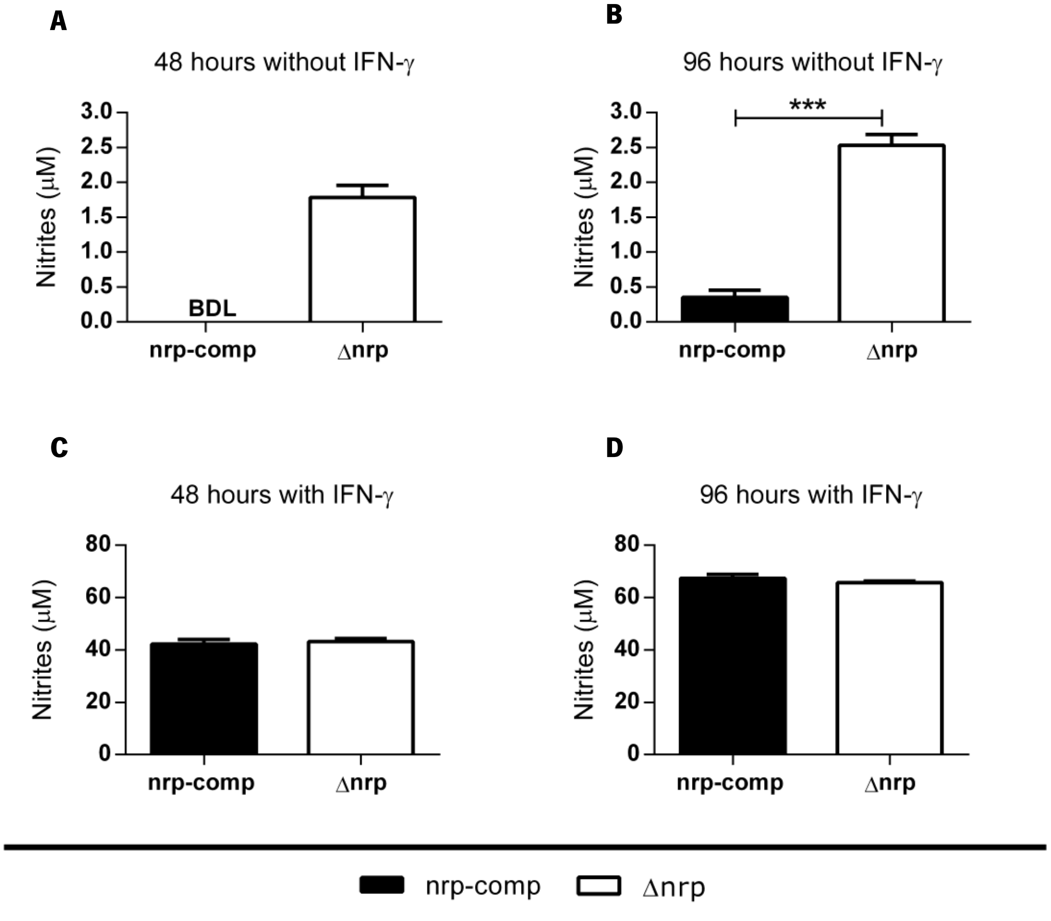

Figure 19: The Δnrp-mutant induced higher nitric oxide production than nrp-complemented Mtb. Nitrites concentration over time in the supernatants of BMDMs infected with either Mtb strain in the absence of IFN-γ at **A)** 48 and **B)** 96 hours and in the presence of IFN-γ at **C)** 48 and **D)** 96 hours post-infection. Data analyzed performing unpaired t tests. Each time-point contains pooled data from 2 separate experiments. ***$p<0.001$

In all, these data may be suggestive that a differential recognition of the Δnrp-mutant is in place, leading to a higher activation of the macrophage. This higher basal activation of the macrophage may in turn explain the previously observed differences in bacterial burdens.

In addition to differences on nitric oxide production, we have also observed differential cytokine production by BMDM after 24 hours of infection. Specifically, we have assessed the concentration of TNF-α and IL-1β, two pro-inflammatory cytokines essential in the immune response to Mtb, and IL-10, a potent anti-inflammatory cytokine (Figure 20). These data show that nrp modulates the activation of innate immune cells. Indeed, BMDMs infected with the Δnrp-mutant produce higher amounts of TNF-α than those infected with the nrp-complemented strain (Figure 20A). Interestingly, the levels of IL-1β and IL-10 remain equivalent between infecting strains (Figure 20B and 20C), suggesting that the difference observed for TNF-α is specific and not due to possible intensity differences intrinsic to the Δnrp-mutant.

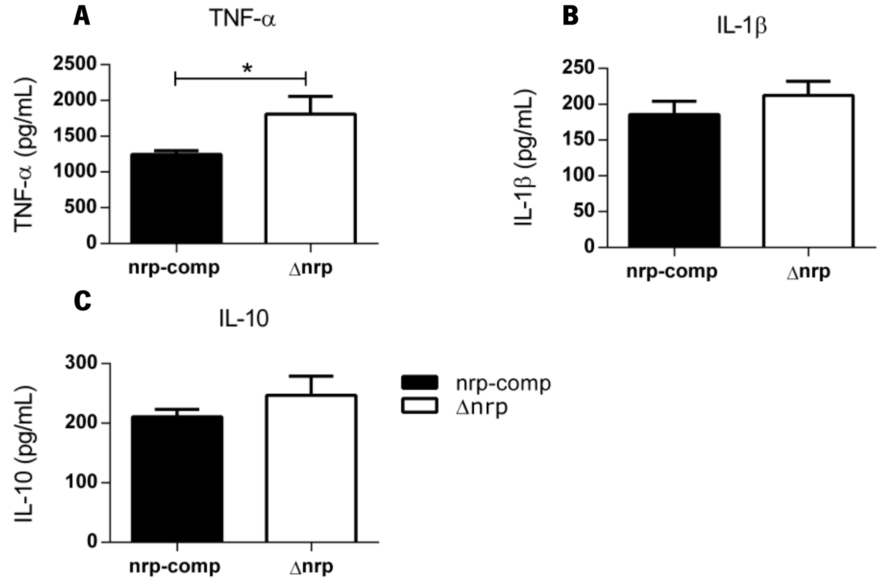

Figure 20: The Δnrp-mutant induced higher production of TNF-α, but not IL-1β or IL-10, than the nrp-complemented Mtb. Inflammatory cytokine concentration in the supernatants of BMDMs 24 hours after infection **A)** TNF-α **B)** IL-1β and **C)** IL-10. Data analyzed performing unpaired t tests. Results from two separate experiments. *p<0.05.

DISCUSSION AND FUTURE PERSPECTIVES

Despite decades of research, TB still remains a leading death cause by infectious disease, second only to the HIV pandemic[3]. Although clear progress has been made in tackling this disease, the fact that for decades little has changed in terms of anti-mycobacterial therapy[4] and that no novel vaccine has proven more effective than BCG[4] are proof that the current knowledge on TB pathophysiology is insufficient to achieve any major breakthrough in this field. The development of tools to genetically manipulate Mtb has allowed us to understand the role of specific pathogen molecules during infection, which may potentially reveal novel therapeutical targets[96,123].

In this work we have defined nrp has a novel Mtb virulence factor. This enzyme is required for optimal establishment of infection, as WT animals infected with the Δnrp-mutant have a better control over infection at least until day 20 post-infection. This superior control subsides by day 30 post-infection, as the lung bacterial burden is similar for animals infected with either the Δnrp-mutant or the nrp-complemented strain. Since our data show that the Δnrp-mutant strain grows at similar rates as the nrp-complemented strain in both rich and minimal media, the reduced growth of the Δnrp-mutant *in vivo* during the innate phase of infection is not associated with an intrinsic growth defect of this strain.

Moreover, and as far as it is possible to assess with the low dose aerosol model, we have not observed any differences between strains regarding infectivity, as both display similar bacterial burdens after 3 days of infection. It would be important to closely monitor the immune response and bacterial burdens during the first weeks of infection, as this would allow us to determine whether the better control over the Δnrp-mutant is associated with an increased susceptibility of this deficient strain to the microbicidal mechanisms of macrophages or whether the specific innate immune response generated against this strain is more efficient at controlling bacterial growth. In this regard, we are currently assessing the bacterial burden and characterizing the innate response of animals infected with Δnrp-mutant or the nrp-complemented strain at time points as early as day 7 and 14 post-infection.

Although nrp expression increases the virulence of Mtb during the innate phase of the infection, allowing bacteria to grow more efficiently in infected macrophages, its expression did not allow evasion of the microbicidal mechanisms triggered by IFN-γ. Indeed, macrophages activated with IFN-γ are equally able to control Mtb regardless of nrp expression. Furthermore, these data go in line with the fact that upon the arrival of an IFN-γ producing T cell response, both Δnrp-mutant and nrp-complemented strains are controlled under a similar stable bacterial burden in WT animals.

Although nrp is not required for the persistence of Mtb during the chronic phase of infection, in its absence mice develop a milder pathological response, as seen by the lower lesioned lung area in these animals in all timepoints assessed. These data suggest that the immune response of the initial phase of infection has important consequences for the immunopathological response generated during the chronic phase of infection. This is important because the pathology induced by Mtb is inflammatory in nature, and this response is responsible for the transmission of Mtb and ultimately to the death of the host[5]. In a clinical point of view, therapeutical interventions during the acute phase of infection may be more effective to prevent transmission of disease and development of pathological consequences to the host.

Our cytometry data clearly showed different dynamics in the cellular immune response elicited by the Δnrp-mutant when compared to the nrp-complemented strain. Overall, we show that in the absence of nrp there is a delay in the recruitment of inflammatory monocytes and in their activation, as well as in the recruitment and activation of CD4+ T cells. An early influx of inflammatory monocytes may actually be detrimental to the host, as they typically lack MyD88 activation and overall microbicidal activity[16,33]. Indeed, it is well described that Mtb exploits CCR2 dependent recruitment of low-microbicidal monocytes[33]. This permissive phenotype of monocytes favors the development of a bacterium-friendly niche, as high accumulation of this cell type around infected macrophages blocks close contact between CD4+ T cells and bacterium-containing cells, thus impeding optimal activation of infected cells[16].

One hypothesis currently being assessed is whether the recruited monocytes have a different phenotype between infecting strains. Specifically, we are screening for the presence of NOS2 in recruited monocytes by flow cytometry. Our hypothesis is that, in the absence of nrp, alveolar macrophages will be differentially activated with higher triggering of MyD88, which in turn would lead to the recruitment of non-permissive monocytes (CD11b+Ly6ChiNOS2+)[33]. These monocytes are described to have higher microbicidal activity, thus allowing for better control of Mtb and potentially explaining the early bacterial load differences between infecting strains. One limitation with this approach is imposed by the difference in IFN-γ and the trend observed in CD4+ T cells by day 20 post-infection between strains. These differences could lead to an increase in NOS2+ inflammatory monocytes in animals infected with the nrp-complemented strain. Therefore experiments are being carried out in both WT and RAG-2 deficient mice.

Another piece of data that fits in this hypothesis is the delayed appearance and stabilization at lower bacterial burden, of the Δnrp-mutant, in the spleen of infected animals. Specifically, it has been shown that bacterial dissemination is facilitated by myeloid cells recruited in a CCR2/CCL2 dependent manner, as these cells are able to move in and out of the local of infection, therefore carrying the bacterium to secondary targets of infection[16]. Our gene expression data showed the lower expression levels of *Ccl2* for day 20 post-infection in the lungs of Δnrp-mutant infected mice. This lower expression may indeed account for the delayed dissemination of the bacterium to the spleen. On the other hand, when dissemination does indeed happen, there is already a robust Mtb-specific T cell response capable of controlling the bacterium's growth[16]. It equally possible that the phenotype observed in the spleen is the result of an impaired ability of the Δnrp-mutant to grow in the specific environment of the spleen. In this case, an intravenous infection should shed light on this issue, as the spleen would be a primary organ of infection, and not a target of dissemination.

A possible confounding factor regarding the flow cytometry data is the marked difference in bacterial burden at day 20 post-infection. One possible hypothesis is that the Δnrp-mutant does indeed induce a differential innate immune response which accounts for the differences in cell recruitment and the lower bacterial burden itself. Another equally valid hypothesis is that the lower numbers of inflammatory monocytes and activated CD4+ T cells are the result of a burden-dependent response. In the future, a high dose aerosol infection will be carried out to account for this variable. In this case, it is expected that by day 20 post-infection the Δnrp-mutant infected animals would have an equivalent bacterial load when compared to the low dose aerosol nrp-complemented infected mice. In this case, assuming that nrp does indeed induce a differential immune response, we should still obtain a discernible phenotype regarding cell recruitment and activation dynamics.

A striking feature that our data has revealed are the differences regarding immunopathology in the lungs of animals infected with either Mtb strain. Even though differences in tissue pathology at day 20 post-infection can easily be attributed to the differential bacterial load, this does not justify the long term differences observed. Indeed, nrp is essential to the development of extensive immunopathology, as seen by the higher percentage of lesioned area in the lungs of animals infected with the nrp-complemented. These differences are even observed in extreme settings, as is the case of moribund IFN-γ deficient animals. Furthermore, in the absence of nrp there is an apparent increased number of individual lesions, although with smaller area. This feature will be quantified in the future, as it may yield important information on the initial events that drive granulomatous lesion formation in the presence or absence of nrp. How these features would translate into Mtb transmission would be an interesting question, as it is hypothesized that some degree of immunopathology must be achieved in order for the bacterium to be expelled from the infected lung[9]. Taking this into consideration, it will be important to assess both host and pathogen molecular players responsible for granuloma formation. One question raised by these structural differences is whether the bacterial TDM, the main inducer of granuloma formation, is in any way altered in the absence of nrp.

One key host factor that would fit with both differences in immunopathology and permissive monocyte recruitment would be the induction of matrix metalloproteinases (MMPs)[124–126]. On one hand, MMP9 is described to be induced upon Mtb's Esx-A delivery to epithelial cells, in turn inducing the recruitment of permissive monocytes through an unknown mechanism, leading to the formation of large lesions and eventually a granuloma-like structure[125]. On the other hand, MMP1 has been reported to breakdown the collagen matrix responsible for granting granulomas structural integrity[124]. If nrp induces the expression of MMP1, the otherwise smaller lesions would be disrupted, allowing Mtb to spread into adjacent tissue, leading to wider lesions. Taking this into consideration, the expression levels of these enzymes will be measured in the future. Another factor that could partially account for the histopathological differences is the type of adaptive response triggered. We are currently phenotyping the adaptive immune response on day 45 post-infection, as by this time the initial differences observed in bacterial burdens should have little impact. One possible scenario would be that in the absence of nrp, the effector T cell response displays less Th17 cell differentiation, which is known to contribute for excessive inflammation. In either case, the fact that IFN-γ deficient animals still present immunopathological differences makes it highly unlikely for a differential Th response to be a defining factor in this phenotype.

Taking into consideration our data, it is evident that nrp exerts its virulence during the innate phase of the immune response, both considering the timeframe in which bacterial burden differences are observed and the survival of animals with severely compromised or absent adaptive immune responses. It is possible that the differential phenotype observed between innate and acquired immune responses may result from a differential expression of nrp throughout infection. Indeed, the bacterium itself may regulate the expression of nrp throughout time, since nrp is the most abundant Mtb protein in the lungs of guinea pigs infected with H37Rv by day 30, whereas it is under detection levels by day 90[34]. Why and whether Mtb does this is a matter of speculation. On one hand, if nrp is no longer required during the chronic phase of infection it would be a poor energetic strategy to waste metabolic resources into an unrequired 2512 amino acid long protein. On the other hand, Mtb may do so to slow disease progression in order to prolong its host's life and increase chances of transmission. In either case, following the transcriptional kinetics of *Nrp* should yield valuable information on which phases of infection this virulence factor is needed. In this line, we are planning to measure the expression of nrp from the bacteria extracted from the lungs of infected animals at different time-points post-infection.

The hypothesis that *nrp* plays a role in the recognition of Mtb by innate immune cells, goes in line with our data. We have seen differences regarding TNF-α and nitrites production in *in vitro* models of macrophage infection. One possible scenario would be that in the absence of nrp Mtb would be more easily recognized by TLR-4, which in turn would lead to RNS production and enhanced TNF-α production in a TIR-domain-containing adapter-inducing interferon-β (TRIF) dependent fashion[88]. However, since there are no discernible differences between WT and TLR-4 deficient animals infected with the Δnrp-mutant this hypothesis is unlikely. It is also unlikely that these differences are due to a differential inflammasome activation, as these should lead to differential production of IL-1β[44], which is not the case. As nrp does not appear to decisively mediate interactions with either TLR-2 or TLR-4, in the future it may be worth to assess if it impacts Mtb recognition by other PRRs (*e.g.* NOD receptors and CLRs).

Considering the phenotype concerning CFUs during *in vitro* infections, they may indeed reflect what is happening inside the phagocyte during *in vivo* infections, as we have observed a consistent result regarding variation in bacterial burden between 4 and 96 hours post-infection in two different types of macrophages. It would be interesting to prolong these experiments beyond 96 hours, as longer time-points may yield more pronounced differences between the Δnrp-mutant and the nrp-complemented strain. However, our experimental setup does not allow for longer time-points, as this would result in macrophage death, thus limiting the accurate determination of intracellular bacterial burden. Alternatively, a phagocytic cell line may be used in the future to overcome this limitation[127].

One particular issue that must be considered in these *in vitro* infections is whether *Nrp* is being expressed at the time of infection, and if not, how long it takes until it is. It is not uncommon for virulence factors that are only required during infection to be downregulated under culture conditions[128], such as those encountered in the inoculum used for these infections. The fact that the absence of nrp leads to a phenotype in macrophage infection, is a good indicator that the nrp-complemented strain is indeed expressing this molecule. However, if nrp expression is delayed, the differences observed by infecting macrophages with either the Δnrp-mutant or the nrp-complemented strain may not fully represent the impact of nrp. Taking this into consideration, in the future it will also be important to assess *Nrp* expression in culture conditions and at different time-points shortly after *in vitro* infection of macrophages.

Taking into consideration the consistent induction of RNS production and our hypothesis of non-permissive NOS2+ monocyte recruitment in the absence of nrp, an experiment with mice infected with the Δnrp-mutant while treated with aminoguanidine[35], a NOS2 inhibitor, is currently being performed. A similar rational will be performed in an *in vitro* setting to determine whether nitric oxide is responsible for the growth deficit of the Δnrp-mutant. RNS production is only one among many possible microbicidal mechanisms that may be behind the phenotype in the absence of nrp. Another mechanism worth exploring *in vitro* that could explain the lower bacterial burden in the absence of nrp, both in *in vivo* and *in vitro* settings, is phagosomal acidification, which can be performed using LysoTracker[36].

One obvious disadvantage on studying a previously uncharacterized enzyme is that there is no knowledge on what it is actually synthesizing, and therefore inferring on the possible differential interactions between host and pathogen is largely an empirical try and error approach. As such, in the future a detailed bioinformatics analysis on this gene and of the remainder of its operon will be performed. Additionally, a characterization of the differences in cell wall lipids between the Δnrp-mutant and the nrp-complemented strain following different experimental conditions (*e.g.* infection, culture) will also be carried out.

Lastly, a thorough characterization of the Δnrp-mutant and nrp-complemented strains growth and resistance under stress conditions will also be performed. These experiments may indicate whether there is a specific stress factor under which nrp is required for Mtb's resistance or whether its cell wall integrity is compromised. These conditions will include nitrosative and oxidative stress, extreme pH, nutrient deprivation, divalent cation deprivation (Fe^{2+}, Mg^{2+}) and detergent exposure[129–134]. With the exception of detergent exposure, these conditions were chosen since they are known to be scenarios encountered by Mtb inside the macrophage[129]. Therefore, failure for the Δnrp-mutant, but not the nrp-complemented strain, to grow in any of these conditions could be a good indicator of the growth-limiting stress factor encountered by the Δnrp-mutant inside the host. Additionally, the detergent exposure experiment will allow us to evaluate whether the absence of nrp leads to a loss of cell wall structural integrity.

To the furthest of our knowledge, the survival phenotype observed in IFN-γ and RAG-2 deficient animals in the absence of nrp is the strongest reported to date. All our data point towards nrp as a virulence factor predominantly during the innate phase of the immune response. Considering our data, nrp inhibition may prove as a suitable drug target against TB, especially in cases of HIV co-infection.

Several parallels may be drawn from infection models of severe adaptive immune deficiency, such as the IFN-γ and RAG-2 deficient animals, with TB-HIV patients. Both have a predominately and prolonged non-protective innate immune response to Mtb, rapidly developing an often lethal severe and disseminated form of TB[3–5]. HIV positive cases still account for more than 25% of deaths due to TB. It is our reasoning that nrp inhibition may slow down disease progression, allowing for a better timeframe to treat these high risk patients.

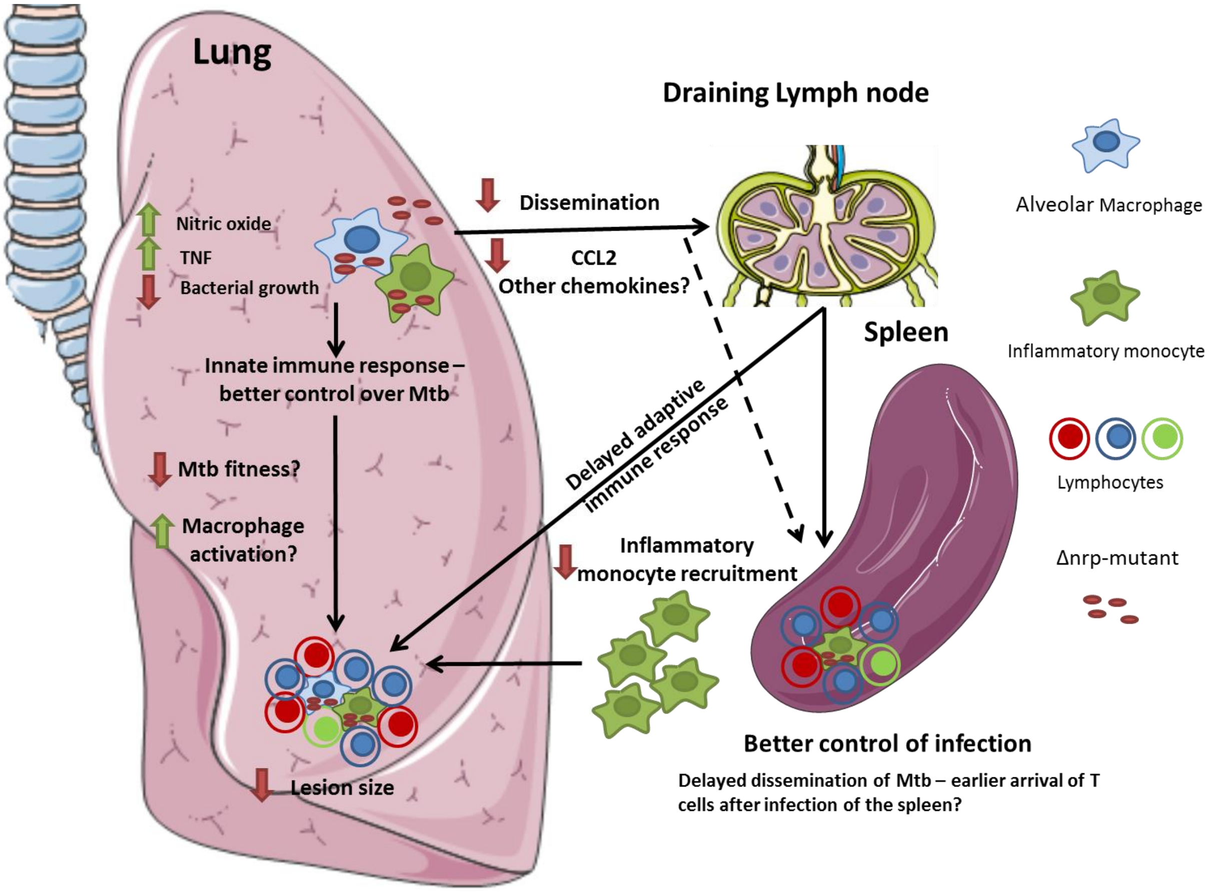
Lung
Draining Lymph node
Dissemination
CCL2
Other chemokines?
Nitric oxide
TNF
Bacterial growth
Innate immune response – better control over Mtb
Mtb fitness?
Macrophage activation?
Delayed adaptive immune response
Inflammatory monocyte recruitment
Spleen
Lesion size
Better control of infection
Delayed dissemination of Mtb – earlier arrival of T cells after infection of the spleen?
Alveolar Macrophage
Inflammatory monocyte
Lymphocytes
Δnrp-mutant

Figure 21: Summary of the main findings and questions resulting of this thesis. Briefly, alveolar macrophages/inflammatory monocytes are differentially activated in the absence of nrp, producing more nitric oxide and TNF. The Δnrp-mutant is better controlled during the innate phase of the immune response, either due to a loss of fitness or due to an increased microbicidal activity of phagocytes. In the absence of nrp, there is a delayed dissemination to peripheral organs and a decreased influx of inflammatory monocytes to the lung, hypothetically in part due to a decreased CCL2 production. This results in a delayed mounting of an adaptive immune response, and consequently a lower influx of lymphocytes to the site of infection. This decreased influx of lymphocytes and inflammatory monocytes is likely to contribute to the smaller size of the lung lesions observed in animals infected with the Δnrp-mutant. Additionally, the delayed detection of Mtb in the spleen and its control under a lower bacterial burden suggests that there is already a protective Mtb-specific T cell response shortly after dissemination to this organ.

In this work we have described nrp as a virulence factor of Mtb, exerting its function mainly during the innate phase of the immune response with important long term pathophysiological consequences. Whether nrp exerts its role by conferring Mtb resistance to microbicidal mechanisms or by differentially activating phagocytes, will be the subject of our future work. We expect that using this type of approach, studying simultaneously host and pathogen factors will benefit greatly our current knowledge of the events taking place in TB.

REFERENCES

1. Lawn, S. D. & Zumla, A. I. Tuberculosis. *Lancet* **378,** 57–72 (2011).

2. Paulson, T. Tuberculosis Epidemiology: A Mortal Foe. *Nat. Outlook* **502,** 2–3 (2013).

3. WHO. Global tuberculosis report 2014. *http://www.who.int/tb/publications/global_report/en/* (2014).

4. Zumla, A., Raviglione, M., Hafner, R. & von Reyn, C. F. Tuberculosis. *N. Engl. J. Med.* **368,** 745–55 (2013).

5. Orme, I. M., Robinson, R. T. & Cooper, A. M. The balance between protective and pathogenic immune responses in the TB-infected lung. *Nat. Immunol.* **16,** 57–63 (2014).

6. Bates, J., Potts, W. & Lewis, M. Epidemiology of Primary Tuberculosis in an Industrial School. *N. Engl. J. Med.* **272,** 714–717 (1965).

7. Wells, W. F., Ratcliffe, H. L. & Grumb, C. On the mechanics of droplet nuclei infection; quantitative experimental air-borne tuberculosis in rabbits. *Am. J. Hyg.* **47,** 11–28 (1948).

8. Cambier, C. J. *et al.* Mycobacteria manipulate macrophage recruitment through coordinated use of membrane lipids. *Nature* **505,** 218–22 (2014).

9. Gold, M. C. *et al.* Human mucosal associated invariant T cells detect bacterially infected cells. *PLoS Biol.* **8,** 1–14 (2010).

10. Flynn, J. & Chan, J. Immunology of Tuberculosis. *Annu. Rev. Immunol.* **19,** 93–129 (2001).

11. North, R. & Jung, Y. Immunity to Tuberculosis. *Annu. Rev. Immunol.* **22,** 599–623 (2004).

12. Bhatt, K. & Salgame, P. Host innate immune response to *Mycobacterium tuberculosis*. *J. Clin. Immunol.* **27,** 347–362 (2007).

13. Kang, D. D., Lin, Y., Moreno, J.-R., Randall, T. D. & Khader, S. a. Profiling early lung immune responses in the mouse model of tuberculosis. *PLoS One* **6,** e16161 (2011).

14. O'Garra, A. *et al.* The Immune Response in Tuberculosis. *Annu. Rev. Immunol.* **25,** 475–527 (2013).

15. Philips, J. a. & Ernst, J. D. Tuberculosis Pathogenesis and Immunity. *Annu. Rev. Pathol. Mech. Dis.* **7,** 353–384 (2012).

16. Schäfer, G., Jacobs, M., Wilkinson, R. J. & Brown, G. D. Non-opsonic recognition of *Mycobacterium tuberculosis* by phagocytes. *J. Innate Immun.* **1,** 231–243 (2009).

17. Medzhitov, R. Recognition of microorganisms and activation of the immune response. *Nature* **449,** 819–826 (2007).

18. Cooper, a M., Mayer-Barber, K. D. & Sher, a. Role of innate cytokines in mycobacterial infection. *Mucosal Immunol.* **4,** 252–60 (2011).

19. Cooper, A. M. *et al.* Mice lacking bioactive IL-12 can generate protective, antigen-specific cellular responses to mycobacterial infection only if the IL-12 p40 subunit is present. *J. Immunol.* **168,** 1322–1327 (2002).

20. Filipe-Santos, O. *et al.* Inborn errors of IL-12/23- and IFN-γ-mediated immunity: molecular, cellular, and clinical features. *Semin. Immunol.* **18,** 347–361 (2006).

21. Alcaïs, A., Fieschi, C., Abel, L. & Casanova, J.-L. Tuberculosis in children and adults: two distinct genetic diseases. *J. Exp. Med.* **202,** 1617–1621 (2005).

22. Alcaïs, A. *et al.* Life-threatening infectious diseases of childhood: Single-gene inborn errors of immunity? *Ann. N. Y. Acad. Sci.* **1214,** 18–33 (2010).

23. Altare, F. *et al.* Interleukin-12 receptor beta1 deficiency in a patient with abdominal tuberculosis. *J. Infect. Dis.* **184,** 231–236 (2001).

24. Boisson-Dupuis, S. *et al.* Il-12rβ1 deficiency in two of fifty children with severe tuberculosis from IRN, MAR, and TUR. *PLoS One* **6,** 1–7 (2011).

25. Ozbek, N. *et al.* Interleukin-12 receptor beta 1 chain deficiency in a child with disseminated tuberculosis. *Clin. Infect. Dis.* **40,** e55–e58 (2005).

26. Watford, W. T., Moriguchi, M., Morinobu, A. & O'Shea, J. J. The biology of IL-12: Coordinating innate and adaptive immune responses. *Cytokine Growth Factor Rev.* **14,** 361–368 (2003).

27. Khader, S. a *et al.* Interleukin 12p40 is required for dendritic cell migration and T cell priming after *Mycobacterium tuberculosis* infection. *J. Exp. Med.* **203,** 1805–1815 (2006).

28. Robinson, R. T. *et al. Mycobacterium tuberculosis* infection induces il12rb1 splicing to generate a novel IL-12Rbeta1 isoform that enhances DC migration. *J. Exp. Med.* **207,** 591–605 (2010).

29. Cooper, a M., Mayer-Barber, K. D. & Sher, a. Role of innate cytokines in mycobacterial infection. *Mucosal Immunol.* **4,** 252–260 (2011).

30. Khader, S. a *et al.* IL-23 compensates for the absence of IL-12p70 and is essential for the IL-17 response during tuberculosis but is dispensable for protection and antigen-specific IFN-gamma responses if IL-12p70 is available. *J. Immunol.* **175,** 788–795 (2005).

31. Leal, I. S., Smedegård, B., Andersen, P. & Appelberg, R. Interleukin-6 and interleukin-12 participate in induction of a type 1 protective T-cell response during vaccination with a tuberculosis subunit vaccine. *Infect. Immun.* **67,** 5747–5754 (1999).

32. Saunders, B. M., Frank, A. a., Orme, I. M. & Cooper, A. M. Interleukin-6 induces early gamma interferon production in the infected lung but is not required for generation of specific immunity to *Mycobacterium tuberculosis* infection. *Infect. Immun.* **68,** 3322–3326 (2000).

33. Ladel, C. H. *et al.* Lethal tuberculosis in interleukin-6-deficient mutant mice. *Infect. Immun.* **65,** 4843–4849 (1997).

34. Flynn, J. *et al.* Tumor necrosis factor-α is required in the protective immune response against *Mycobacterium tuberculosis* in mice. *Immunity* **2,** 561–572 (1995).

35. Bean, a G. *et al.* Structural deficiencies in granuloma formation in TNF gene-targeted mice underlie the heightened susceptibility to aerosol *Mycobacterium tuberculosis* infection, which is not compensated for by lymphotoxin. *J. Immunol.* **162,** 3504–3511 (1999).

36. Kaneko, H. *et al.* Role of tumor necrosis factor-alpha in Mycobacterium-induced granuloma formation in tumor necrosis factor-alpha-deficient mice. *Lab. Invest.* **79,** 379–386 (1999).

37. Harris, J. & Keane, J. How tumour necrosis factor blockers interfere with tuberculosis immunity. *Clin. Exp. Immunol.* **161,** 1–9 (2010).

38. Miller, E. a. & Ernst, J. D. Anti-TNF immunotherapy and tuberculosis reactivation: Another mechanism revealed. *J. Clin. Invest.* **119,** 1079–1082 (2009).

39. Keane, J. *et al.* Tuberculosis Associated with Infliximab, A Tumor Necrosis Factor alpha-Neutralizing Agent. *N. Engl. J. Med.* **345,** 1098–1104 (2001).

40. Miller, E. a. & Ernst, J. D. Illuminating the Black Box of TNF Action in Tuberculous Granulomas. *Immunity* **29,** 175–177 (2008).

41. Lin, P. L., Plessner, H. L., Voitenok, N. N. & Flynn, J. L. Tumor necrosis factor and tuberculosis. *J. Investig. Dermatol. Symp. Proc.* **12,** 22–25 (2007).

42. Juffermans, N. P. *et al.* Interleukin-1 signaling is essential for host defense during murine pulmonary tuberculosis. *J. Infect. Dis.* **182,** 902–908 (2000).

43. Sugawara, I., Yamada, H., Hua, S. & Mizuno, S. Role of interleukin (IL)-1 type 1 receptor in mycobacterial infection. *Microbiol. Immunol.* **45,** 743–750 (2001).

44. Mayer-Barber, K. D. *et al.* Caspase-1 independent IL-1beta production is critical for host resistance to *Mycobacterium tuberculosis* and does not require TLR signaling in vivo. *J. Immunol.* **184,** 3326–3330 (2010).

45. Mayer-Barber, K. D. *et al.* Innate and Adaptive Interferons Suppress IL-1a and IL-1b Production by Distinct Pulmonary Myeloid Subsets during *Mycobacterium tuberculosis* Infection. *Immunity* **35,** 1023–1034 (2011).

46. Mayer-Barber, K. D. *et al.* Host-directed therapy of tuberculosis based on interleukin-1 and type I interferon crosstalk. *Nature* **511,** 99–103 (2014).

47. Behar, S. M., Divangahi, M. & Remold, H. G. Evasion of innate immunity by *Mycobacterium tuberculosis*: is death an exit strategy? *Nat. Rev. Microbiol.* **8,** 668–674 (2010).

48. Divangahi, M., Desjardins, D., Nunes-Alves, C., Remold, H. G. & Behar, S. M. Eicosanoid pathways regulate adaptive immunity to *Mycobacterium tuberculosis*. *Nat. Immunol.* **11,** 751–758 (2010).

49. Harizi, H., Corcuff, J. B. & Gualde, N. Arachidonic-acid-derived eicosanoids: roles in biology and immunopathology. *Trends Mol. Med.* **14,** 461–469 (2008).

50. Divangahi, M. *et al. Mycobacterium tuberculosis* evades macrophage defenses by inhibiting plasma membrane repair. *Nat. Immunol.* **10,** 899–906 (2009).

51. Bafica, A. *et al.* Host control of *Mycobacterium tuberculosis* is regulated by 5-lipoxygenase–dependent lipoxin production. *J. Clin. Invest.* **115,** 1601–1606 (2005).

52. Tobin, D. M. *et al.* The lta4h Locus Modulates Susceptibility to Mycobacterial Infection in Zebrafish and Humans. *Cell* **140,** 717–730 (2010).

53. Herb, F. *et al.* ALOX5 variants associated with susceptibility to human pulmonary tuberculosis. *Hum. Mol. Genet.* **17,** 1052–1060 (2008).

54. Behar, S. M. & Sassetti, C. M. Immunology: Fixing the odds against tuberculosis. *Nature* **511,** 39–40 (2014).

55. Friedland, J. S. Targeting the Inflammatory Response in Tuberculosis. *N. Engl. J. Med.* **371,** 1354–1356 (2014).

56. Ottenhoff, T. H. M. *et al.* Genome-Wide Expression Profiling Identifies Type 1 Interferon Response Pathways in Active Tuberculosis. *PLoS One* **7,** e45839 (2012).

57. Ordway, D. *et al.* The hypervirulent *Mycobacterium tuberculosis* strain HN878 induces a potent TH1 response followed by rapid down-regulation. *J. Immunol.* **179,** 522–531 (2007).

58. Stanley, S. a, Johndrow, J. E., Manzanillo, P. & Cox, J. S. The Type I IFN response to infection with *Mycobacterium tuberculosis* requires ESX-1-mediated secretion and contributes to pathogenesis. *J. Immunol.* **178,** 3143–3152 (2007).

59. Manuscript, A. *Mycobacterium tuberculosis* triggers host type I interferon signaling to regulatue IL-1B production in human macrophages. *J. Immunol.* **29,** 997–1003 (2011).

60. Slight, S. R. & Khader, S. a. Chemokines shape the immune responses to tuberculosis. *Cytokine Growth Factor Rev.* **24,** 105–113 (2013).

61. Lu, B. *et al.* Abnormalities in monocyte recruitment and cytokine expression in monocyte chemoattractant protein 1-deficient mice. *J. Exp. Med.* **187,** 601–608 (1998).

62. Scott, H. M. & Flynn, J. L. *Mycobacterium tuberculosis* in Chemokine Receptor 2-Deficient Mice : Influence of Dose on Disease Progression Mycobacterium tuberculosis in Chemokine Receptor 2-Deficient Mice : Influence of Dose on Disease Progression. **70,** 5946–5954 (2002).

63. Peters, W. *et al.* Chemokine receptor 2 serves an early and essential role in resistance to *Mycobacterium tuberculosis*. *Proc. Natl. Acad. Sci. U. S. A.* **98,** 7958–7963 (2001).

64. Kipnis, A., Basaraba, R. J., Orme, I. M. & Cooper, A. M. Role of chemokine ligand 2 in the protective response to early murine pulmonary tuberculosis. *Immunology* **109,** 547–551 (2003).

65. Feng, W. *et al.* CCL2 − 2518 (A / G) polymorphisms and tuberculosis susceptibility : a meta-analysis. *Int. J. Tuberc. Lung Dis.* **16,** 150–156 (2011).

66. Vesosky, B., Rottinghaus, E. K., Stromberg, P., Turner, J. & Beamer, G. CCL5 participates in early protection against *Mycobacterium tuberculosis*. *J. Leukoc. Biol.* **87,** 1153–1165 (2010).

67. Kahnert, A. *et al. Mycobacterium tuberculosis* triggers formation of lymphoid structure in murine lungs. *J. Infect. Dis.* **195,** 46–54 (2007).

68. Olmos, S., Stukes, S. & Ernst, J. D. Ectopic activation of *Mycobacterium tuberculosis*-specific CD4+ T cells in lungs of CCR7-/- mice. *J. Immunol.* **184,** 895–901 (2010).

69. Khader, S. a *et al.* In a murine tuberculosis model, the absence of homeostatic chemokines delays granuloma formation and protective immunity. *J. Immunol.* **183,** 8004–8014 (2009).

70. Wolf, A. J. *et al. Mycobacterium tuberculosis* infects dendritic cells with high frequency and impairs their function in vivo. *J. Immunol.* **179,** 2509–2519 (2007).

71. Havlir, D. V. *et al.* Timing of Antiretroviral Therapy for HIV-1 Infection and Tuberculosis. *N. Engl. J. Med.* **365,** 1482–1491 (2011).

72. Abdool Karim, S. S. *et al.* Integration of antiretroviral therapy with tuberculosis treatment. *N. Engl. J. Med.* **365,** 1492–501 (2011).

73. Nandi, B. & Behar, S. M. Regulation of neutrophils by interferon- limits lung inflammation during tuberculosis infection. *J. Exp. Med.* **208,** 2251–2262 (2011).

74. Swain, S. L., McKinstry, K. K. & Strutt, T. M. Expanding roles for CD4+ T cells in immunity to viruses. *Nat. Rev. Immunol.* **12,** 136–148 (2012).

75. Lazarevic, V., Glimcher, L. H. & Lord, G. M. T-bet: a bridge between innate and adaptive immunity. *Nat. Rev. Immunol.* **13,** 777–89 (2013).

76. Jung, Y.-J., Ryan, L., LaCourse, R. & North, R. J. Properties and protective value of the secondary versus primary T helper type 1 response to airborne *Mycobacterium tuberculosis* infection in mice. *J. Exp. Med.* **201,** 1915–1924 (2005).

77. Flynn, J. L. *et al.* An essential role for interferon gamma in resistance to *Mycobacterium tuberculosis* infection. *J. Exp. Med.* **178,** 2249–2254 (1993).

78. Cirillo, S. L. G. *et al.* Protection of *Mycobacterium tuberculosis* from reactive oxygen species conferred by the mel2 locus impacts persistence and dissemination. *Infect. Immun.* **77,** 2557–2567 (2009).

79. Ehrt, S. *et al.* Reprogramming of the macrophage transcriptome in response to interferon-gamma and *Mycobacterium tuberculosis*: signaling roles of nitric oxide synthase-2 and phagocyte oxidase. *J. Exp. Med.* **194,** 1123–1140 (2001).

80. John, C., Yun, X., Richar S., M. & Barry R., B. Killing of Virulent *Mycobacterium tuberculosis* by Reactive Nitrogen Intermediates Produced by Activated Murine Macrophages. *J. Exp. Med.* **175,** 1111–1122 (1992).

81. Repique, C. J. *et al.* Susceptibility of mice deficient in the MHC class II transactivator to infection with *Mycobacterium tuberculosis*. *Scand J Immunol* **58,** 15–22 (2003).

82. Mogues, T., Goodrich, M. E., Ryan, L., LaCourse, R. & North, R. J. The relative importance of T cell subsets in immunity and immunopathology of airborne *Mycobacterium tuberculosis* infection in mice. *J. Exp. Med.* **193,** 271–280 (2001).

83. Torrado, E. & Cooper, A. M. IL-17 and Th17 cells in tuberculosis. *Cytokine Growth Factor Rev.* **21,** 455–462 (2010).

84. Okamoto Yoshida, Y. *et al.* Essential role of IL-17A in the formation of a mycobacterial infection-induced granuloma in the lung. *J. Immunol.* **184,** 4414–4422 (2010).

85. Cruz, A. *et al.* Pathological role of interleukin 17 in mice subjected to repeated BCG vaccination after infection with *Mycobacterium tuberculosis*. *J. Exp. Med.* **207,** 1609–1616 (2010).

86. Umemura, M. *et al.* IL-17-Mediated Regulation of Innate and Acquired Immune Response against Pulmonary *Mycobacterium bovis* Bacille Calmette-Guérin Infection. *J. Immunol.* **178,** 3786–3796 (2007).

87. Comas, I. *et al.* Out-of-Africa migration and Neolithic coexpansion of *Mycobacterium tuberculosis* with modern humans. *Nat. Genet.* **45,** 1176–1182 (2013).

88. Carmona, J. *et al. Mycobacterium tuberculosis* Strains Are Differentially Recognized by TLRs with an Impact on the Immune Response. *PLoS One* **8,** e67277 (2013).

89. Portevin, D., Gagneux, S., Comas, I. & Young, D. Human macrophage responses to clinical isolates from the *Mycobacterium tuberculosis* complex discriminate between ancient and modern lineages. *PLoS Pathog.* **7,** e1001307 (2011).

90. Krishnan, N. *et al. Mycobacterium tuberculosis* Lineage Influences Innate Immune Response and Virulence and Is Associated with Distinct Cell Envelope Lipid Profiles. *PLoS One* **6,** e23870 (2011).

91. Wang, C. *et al.* Innate immune response to *Mycobacterium tuberculosis* Beijing and other genotypes. *PLoS One* **5,** e13594 (2010).

92. Lopez-Marin, L. M. Nonprotein structures from mycobacteria: Emerging actors for tuberculosis control. *Clin. Dev. Immunol.* **2012,** (2012).

93. Asselineau, J. & Lanéelle, G. Mycobacterial lipids: a historical perspective. *Front. Biosci.* **3,** e164–e174 (1998).

94. Abdallah, A. M. *et al.* Type VII secretion–mycobacteria show the way. *Nat. Rev. Microbiol.* **5,** 883–891 (2007).

95. Cole, S. T. *et al.* Deciphering the biology of *Mycobacterium tuberculosis* from the complete genome sequence. *Nature* **393,** 537–544 (1998).

96. Larsen, M. H., Biermann, K., Tandberg, S., Hsu, T. & Jacobs, W. R. Genetic Manipulation of *Mycobacterium tuberculosis. Curr. Protoc. Microbiol.* **Chapter 10,** (2007).

97. Glickman, M. S., Cox, J. S. & Jacobs, W. R. A novel mycolic acid cyclopropane synthetase is required for cording, persistence, and virulence of *Mycobacterium tuberculosis*. *Mol. Cell* **5,** 717–727 (2000).

98. Dao, D. N. *et al.* Mycolic acid modification by the mmaA4 gene of *M. tuberculosis* modulates IL-12 production. *PLoS Pathog.* **4,** e1000081 (2008).

99. Rao, V., Gao, F., Chen, B., Jacobs, W. R. & Glickman, M. S. Trans-cyclopropanation of mycolic acids on trehalose dimycolate suppresses *Mycobacterium tuberculosis*-induced inflammation and virulence. *J. Clin. Invest.* **116,** 1660–1667 (2006).

100. Rao, V., Fujiwara, N., Porcelli, S. a & Glickman, M. S. *Mycobacterium tuberculosis* controls host innate immune activation through cyclopropane modification of a glycolipid effector molecule. *J. Exp. Med.* **201,** 535–543 (2005).

101. Goren, M. B., Brokl, O. & Schaefer, W. B. Lipids of putative relevance to virulence in *Mycobacterium tuberculosis*: Phthiocerol dimycocerosate and the attenuation indicator lipid. *Infect. Immun.* **9,** 150–158 (1974).

102. Rousseau, C. *et al.* Production of phthiocerol dimycocerosates protects *Mycobacterium tuberculosis* from the cidal activity of reactive nitrogen intermediates produced by macrophages and modulates the early immune response to infection. *Cell. Microbiol.* **6,** 277–287 (2004).

103. Astarie-Dequeker, C. *et al.* Phthiocerol dimycocerosates of *M. tuberculosis* participate in macrophage invasion by inducing changes in the organization of plasma membrane lipids. *PLoS Pathog.* **5,** (2009).

104. Day, T. a. *et al. Mycobacterium tuberculosis* Strains Lacking Surface Lipid Phthiocerol Dimycocerosate Are Susceptible to Killing by an Early Innate Host Response. *Infect. Immun.* **82,** 5214–5222 (2014).

105. Converse, S. E. *et al.* MmpL8 is required for sulfolipid-1 biosynthesis and *Mycobacterium tuberculosis* virulence. *Proc. Natl. Acad. Sci. U. S. A.* **100,** 6121–6126 (2003).

106. Nabatov, A. a., Hatzis, P., Rouschop, K. M. a, Van Diest, P. & Vooijs, M. Hypoxia inducible NOD2 interacts with 3-O-sulfogalactoceramide and regulates vesicular homeostasis. *Biochim. Biophys. Acta - Gen. Subj.* **1830,** 5277–5286 (2013).

107. Gilmore, S. a. *et al.* Sulfolipid-1 biosynthesis restricts *Mycobacterium tuberculosis* growth in human macrophages. *ACS Chem. Biol.* **7,** 863–870 (2012).

108. Rousseau, C. *et al.* Sulfolipid Deficiency Does Not Affect the Virulence of *Mycobacterium tuberculosis* H37Rv in Mice and Guinea Pigs Sulfolipid Deficiency Does Not Affect the Virulence of Mycobacterium tuberculosis H37Rv in Mice and Guinea Pigs. *Infect. Immun.* **71,** 4684–4690 (2003).

109. Domenech, P. *et al.* The role of MmpL8 in sulfatide biogenesis and virulence of *Mycobacterium tuberculosis*. *J. Biol. Chem.* **279,** 21257–21265 (2004).

110. Zhang, L., English, D. & Andersen, B. R. Activation of Human Neutrophils by *Mycobacterium tuberculosis* derived Sulfolipid-1. *J. Immunol* **146,** 2730–2736 (1991).

111. Murry, J. P., Pandey, A. K., Sassetti, C. M. & Rubin, E. J. Characterization of Sulfolipids of *Mycobacterium tuberculosis* H37Rv by Multiple-stage Linear Ion-trap High Resolution Mass Spectrometry with Electrospray Ionization Reveals that Family of Sulfolipid II predominates. *J. Infect. Dis.* **29,** 997–1003 (2012).

112. Fratti, R. a., Backer, J. M., Gruenberg, J., Corvera, S. & Deretic, V. Role of phosphatidylinositol 3-kinase and Rab5 effectors in phagosomal biogenesis and mycobacterial phagosome maturation arrest. *J. Cell Biol.* **154,** 631–644 (2001).

113. Mishra, A. K., Driessen, N. N., Appelmelk, B. J. & Besra, G. S. Lipoarabinomannan and related glycoconjugates: Structure, biogenesis and role in *Mycobacterium tuberculosis* physiology and host-pathogen interaction. *FEMS Microbiol. Rev.* **35,** 1126–1157 (2011).

114. Mishra, A. K. *et al.* Differential arabinan capping of lipoarabinomannan modulates innate immune responses and impacts T helper cell differentiation. *J. Biol. Chem.* **287,** 44173–44183 (2012).

115. Stoop, E. J. M. *et al.* Mannan core branching of lipo(arabino)mannan is required for mycobacterial virulence in the context of innate immunity. *Cell. Microbiol.* **15,** 2093–2108 (2013).

116. Wang, F., Langley, R., Gulten, G., Wang, L. & Sacchettini, J. C. Identification of a type III thioesterase reveals the function of an operon crucial for Mtb virulence. *Chem. Biol.* **14,** 543–51 (2007).

117. Raman, S. *et al.* Mycobacterium tuberculosis SigM positively regulates Esx secreted protein and nonribosomal peptide synthetase genes and down regulates virulence-associated surface lipid synthesis. *J. Bacteriol.* **188,** 8460–8468 (2006).

118. Mawuenyega, K. G. *et al. Mycobacterium tuberculosis* Functional Network Analysis by Global Subcellular Protein Profiling. *Mol. Biol. Cell* **16,** 396–404 (2005).

119. Griffin, J. E. *et al.* High-resolution phenotypic profiling defines genes essential for mycobacterial growth and cholesterol catabolism. *PLoS Pathog.* **7,** e1002251 (2011).

120. Sassetti, C. M., Boyd, D. H. & Rubin, E. J. Genes required for mycobacterial growth defined by high density mutagenesis. *Mol. Microbiol.* **48,** 77–84 (2003).

121. Kruh, N. a, Troudt, J., Izzo, A., Prenni, J. & Dobos, K. M. Portrait of a pathogen: the *Mycobacterium tuberculosis* proteome in vivo. *PLoS One* **5,** e13938 (2010).

122. Massey, S. *et al.* Comparative *Burkholderia pseudomallei* natural history virulence studies using an aerosol murine model of infection. *Sci. Rep.* **4,** 4305 (2014).

123. Forrellad, M. A. *et al.* Virulence factors of the *Mycobacterium tuberculosis* complex. *Virulence* **4,** 3–66 (2013).

124. Salgame, P. MMPs in tuberculosis: Granuloma creators and tissue destroyers. *J. Clin. Invest.* **121,** 1686–1688 (2011).

125. Volkman, H. E. *et al.* Tuberculous granuloma induction via interaction of a bacterial secreted protein with host epithelium. *Science* **327,** 466–469 (2010).

126. Price, N. M. *et al.* Identification of a matrix-degrading phenotype in human tuberculosis in vitro and in vivo. *J. Immunol.* **166,** 4223–4230 (2001).

127. Theus, S. a, Cave, M. D. & Eisenach, K. D. Intracellular macrophage growth rates and cytokine profiles of *Mycobacterium tuberculosis* strains with different transmission dynamics. *J Infect Dis* **191,** 453–460 (2005).

128. Talaat, A. M., Lyons, R., Howard, S. T. & Johnston, S. A. The temporal expression profile of *Mycobacterium tuberculosis* infection in mice. *Proc. Natl. Acad. Sci. U. S. A.* **101,** 4602–4607 (2004).

129. Garg, R. *et al.* The Conserved Hypothetical Protein Rv0574c Is Required for Cell Wall Integrity, Stress Tolerance, and Virulence of *Mycobacterium tuberculosis*. *Infect. Immun.* **83,** 120–129 (2015).

130. Goodsmith, N. *et al.* Disruption of an *M. tuberculosis* Membrane Protein Causes a Magnesium-dependent Cell Division Defect and Failure to Persist in Mice. *PLOS Pathog.* **11,** e1004645 (2015).

131. Simeone, R. *et al.* Cytosolic Access of *Mycobacterium tuberculosis*: Critical Impact of Phagosomal Acidification Control and Demonstration of Occurrence In Vivo. *PLOS Pathog.* **11,** e1004650 (2015).

132. Khare, G., Reddy, P. V., Sidhwani, P. & Tyagi, A. K. KefB inhibits phagosomal acidification but its role is unrelated to *M. tuberculosis* survival in host. *Sci. Rep.* **3,** 3527 (2013).

133. Gengenbacher, M., Rao, S. P. S., Pethe, K. & Dick, T. Nutrient-starved, non-replicating *Mycobacterium tuberculosis* requires respiration, ATP synthase and isocitrate lyase for maintenance of ATP homeostasis and viability. *Microbiology* **156,** 81–87 (2010).

134. Lamichhane, G. *Mycobacterium tuberculosis* response to stress from reactive oxygen and nitrogen species. *Front. Microbiol.* **2,** 1–2 (2011).